Modeling an angiogenesis treatment after a myocardial infarction

Literature study

L.Y.D. Crapts

Supervisor:
Dr.ir. F.J. Vermolen
Dr. J.K. Ryan

March 29, 2012

Contents

Chapter 1

Introduction

The goal of this research is to learn more about the amount of stem cells that has to be injected into the wound of the heart after a heart attack, aiming to avoid the formation of scar tissue.

This literature study first discusses the medical (biological) background of the heart attack and the stem cell method. Then two mathematical models are introduced and some mathematical analysis is done in order to draw some preliminary conclusions. One of the models will be chosen to use for our further research.

Then we apply several numerical methods to our model in order to understand how the model works and how the process called angiogenesis is being triggered by injection of the stem cells. The methods Streamline Upwind Petrov-Galerkin and discontinuous Galerkin (with limiting) are introduced and some results are obtained using these methods to the (perturbed) advection equation.

This has been done for the one dimensional model where we assumed the wound of the heart to be symmetric around the center, which is located at the origin in our results.

Chapter 2

Biological background

2.1 Myocardial infarction

A myocardial infarction, or commonly called a 'heart attack', is often the result of a blockage in the coronary artery after the artery has been narrowed. In this chapter we treat events before and after the myocardial infarction and we start with the narrowing of the arteries.

The condition in which an artery wall thickes as a result of the accumulation of fatty acids and cholesterol is called atherosclerosis (the layer of these fatty acids and cholesterol is named plaque) [1]. Bad lifestyle like

- smoking,
- alcohol,
- obesity,
- lack of exercise,
- stress,

and genetic deficiencies like

- cardiovascular disease,
- diabetes,
- high blood pressure,

are risk factors for atherosclerosis. When atherosclerosis occurs, the passage of blood through the arteries will be smaller and the blood stream to the heart muscle decreases. Even a small blood clot can now be a blockage of the (coronary) artery and therefore cause a myocardial infarction. Such a blood clot can be formed near and due to a tear in the wall of a artery which is caused by the atherosclerosis. In Figure 2.1.1 atherosclerosis and clotting blood are shown.

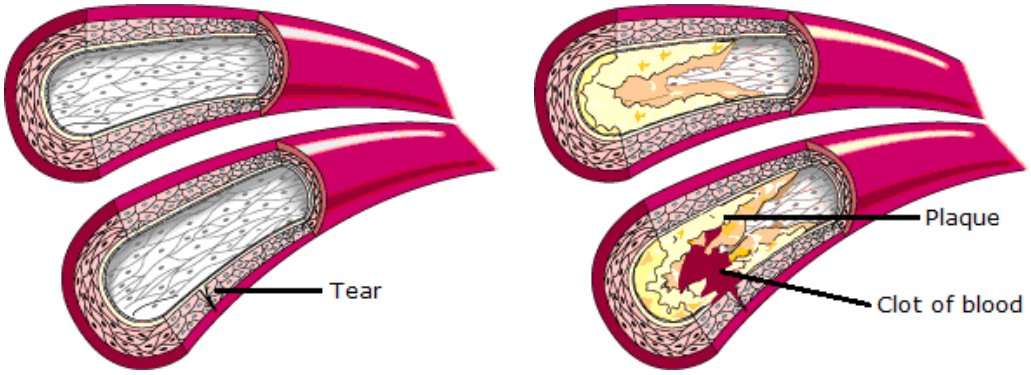

(a) Two arteries without atherosclerosis, where the lowest artery has a tear in the artery wall.

(b) Both arteries with atherosclerosis, where a clot of blood is formed near the tear.

Figure 2.1.1: *Atherosclerosis in the arteries* [1].

At the moment of such a blockage, the blood supply to the heart is poor and therefore the supply of oxygen and nutrients is insufficient. Due to the insufficient supply, a myocardial infarction occures where the infarction represents the decease of myocardial tissue (death of heart cells in the heart muscle).

The dead cells in the affected heart region, cause fibroblasts to excessively secrete collagen, which results into scar tissue with stiff mechanical properties. These mechanical properties will result into a higher resistence of the pump function to be carried by the heart muscle. This higher resistence, which frustrates the pump function, will result into growth of the present myocyte cells as a natural reaction of all muscle cells to hard labor. As a result, the muscle cells will decease more rapidly than in circumstances without a heart attack, which eventually will result into heart failure, and hence in death of the patient.

2.2 Angiogenesis

In this section we give a introduction to angiogenesis [2]. In short, angiogenesis is the formation of new blood vessels from existing blood vessels. For example, angiogenesis is important in the process of wound healing and in the present application, angiogenesis is stimulated to reduce amount of fibrosis at locations suffering from a myocardial infarction and hence to reduce the risk of hart failure after a myocardial infarction.

The formation of new blood vessels happens due to angiogenic factors, like hormones, which are secreted by neighboring cells. The angiogenic factors stimulate the growth, division and mobility of neighboring endothelial cells (EC), which constitute the walls of the blood vessels. By doing this, the endothelial cells will split at the tops of the capillaries such that the capillaries grow and branch off.

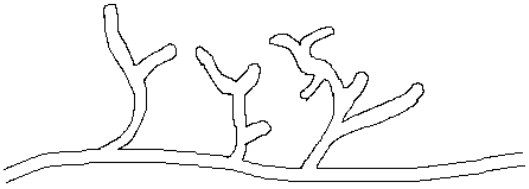

Figure 2.2.1: *Capillaries branching off.*

Cell-division is a complicated biological process. At the moment the angiogenic factors are stimulating the endothelial cells, these endothelial cells secrete enzymes which degrade their basal membrane/lamina (a thin acellulair layer around a capillary which separates different types of tissue) and the extracellular matrix (ECM, acellular part that provides mechanical support to cells). After 'breaking down' the basale membrane and the extracellular matrix the endothelial cells have the possibility to branch off. After branching off, the endothelial cells will form a new basale membrane around themselves.

After forming new vessels and new capillary tips they do not necessarily branch off again. It is also possible that neighboring vessels fuse together and form a new loop. This process is called anastomosis. It is also possible that a tip of a capillary fuses together with another vessel.

(a) Tips fusing together. (b) Tip of capillary and vessel fusing together.

Figure 2.2.2: *Two modes of anastomosis.*

2.3 New treatment

In Chapter 2.1, we described the consequences and the events that occur after a myocardial infarction. In order to prevent the formation of scar tissue, and therewith to lower the possibility of heart failure, a new treatment is currently being investigated. With this treatment, stem cells are injected onto damaged regions of the heart (the so called wound). These stem cells will secrete, among many others, the growth factor TG-beta, which enhances angiogenesis (see Chapter 2.2) in the sense that

- endothelial cells are provoked to move towards the 'wound' (chemotaxis);

- endothelial cells are provoked to divide, by which new arteries are formed and extended as a result of proliferation of endothelial cells.

After the enhanced angiogenesis, vessels have been formed in the damaged part of the heart aiming at avoiding the formation of scar tissue.

Chapter 3

Mathematical Model

In this chapter we introduce the mathematical model to describe the angiogenesis. This is based on a model for tumor angiogenesis from [2]. The model for tumor angiogenesis takes into account an attractant, the change in capillary tip density and the change in the vessel density. Further, we have an equation for the stem cell density since the injected stem cells excrete the attractant TG-beta. In this report, the area of the wound is denoted by Ω_w, while the total domain we observe around the wound is denoted by Ω.

3.1 Stem cell density

To stimulate the angiogenesis around the specific area of the heart an amount of stem cells is injected once. These stem cells secrete the attractant TG-beta. Due to reactions the amount of stem cells will decrease exponentially in time. Therefore the equation for the amount of stem cells is given by

$$\frac{\partial m}{\partial t} = -\beta_1 m, \tag{3.1.1}$$

with coefficient β_1 and where we have the initial injected amount of stem cells

$$m(x,0) = \begin{cases} m_0 & x \in \Omega_m \\ 0 & x \in \Omega \backslash \Omega_m \end{cases} . \tag{3.1.2}$$

The dimension of the coefficient is

- $\dim(\beta_1) = \left[\frac{1}{s}\right]$.

3.2 Concentration TG-beta

As an addition to the equation for the concentration attractant in [2] we now have an injected source that secretes the attractant. The equation for the concentration TG-beta

now becomes

$$\frac{\partial c}{\partial t} - \underbrace{D_1 \frac{\partial^2 c}{\partial x^2}}_{\substack{\text{random}\\ \text{walk}}} + \lambda c = \alpha m, \tag{3.2.1}$$

with diffusion coefficient D_1 and the coefficient λ for the decrease of attractant to due reactions with other substances [3]. Since our left boundary is the center of the wound we actually have a symmetric problem so the concentration TG-beta has initial conditions

$$c(x, 0) = 0, \tag{3.2.2}$$

and Neumann boundary conditions

$$\frac{\partial c}{\partial x}(0, t) = \frac{\partial c}{\partial x}(1, t) = 0. \tag{3.2.3}$$

The dimensions of the coefficients are

- $\dim(D_1) = \left[\frac{mm^2}{s}\right]$,
- $\dim(\alpha) = \left[\frac{mol}{s}\right]$,
- $\dim(\lambda) = \left[\frac{1}{s}\right]$.

3.3 Capillary tip density

Since the source of TG-beta, the stem cells, has already been taken into account in the equation for the concentration TG-beta, the source plays only an indirect role in the density of the capillary tips. Therefore the equation from [2] is also applicable in our case. Hence the equation for the capillary tip density is given by

$$\frac{\partial n}{\partial t} + \underbrace{\chi_1 \frac{\partial}{\partial x}\left(n \frac{\partial c}{\partial x}\right)}_{\text{chemotaxis}} - \underbrace{D_2 \frac{\partial^2 n}{\partial x^2}}_{\substack{\text{random}\\ \text{walk}}} = \underbrace{\alpha_0 \rho c}_{\substack{\text{bifur-}\\ \text{cation}\\ \text{at}\\ \text{vessels}}} + \underbrace{\alpha_1 H(c - \hat{c}) n c}_{\substack{\text{bifurcation}\\ \text{of tips}}} - \underbrace{\beta_2 n \rho}_{\substack{\text{anasto-}\\ \text{mosis}}}, \tag{3.3.1}$$

where χ_1 is the chemotaxis coefficient, so the influence of attractant TG-beta to the mobility of the capillary tips, and D_2 the diffusion coefficient. Further we have α_0 as coefficient for the first type of angiogenesis, which is an increase of capillary tips because they branch of from blood vessels as a reaction to the attractant TG-beta. Further, we have α_1 as the coefficient of the second type of angiogenesis where a threshold of attractant, $\hat{c}$, causes capillary tips to branch off. Finally we have β_2 as the coefficient for the decrease of capillary tips because of the joining of tips-sprouts. This process is called anastomosis [3].
Note that $H(c - \hat{c})$ is the Heaviside term defined by

$$H(c-\hat{c}) = \begin{cases} 1, & c \geq \hat{c}, \\ 0, & c < \hat{c}. \end{cases} \tag{3.3.2}$$

Initially there are no capillary tips, so

$$n(x,0) = 0, \tag{3.3.3}$$

and again, because our problem is symmetric, we have Neumann conditions on the boundary

$$\chi_1 n \frac{\partial c}{\partial x} - D_2 \frac{\partial n}{\partial x}\bigg|_{x=0} = \chi_1 n \frac{\partial c}{\partial x} - D_2 \frac{\partial n}{\partial x}\bigg|_{x=1} = 0,$$

such that using boundary conditions (3.2.3)

$$\frac{\partial n}{\partial x}(0,t) = \frac{\partial n}{\partial x}(1,t) = 0. \tag{3.3.4}$$

Again with the dimensions of the coefficients

- $\dim(\chi_1) = \left[\frac{mm^2}{s} \cdot mm^3\right]$,
- $\dim(D_2) = \left[\frac{mm^2}{s}\right]$,
- $\dim(\alpha_0) = \left[\frac{mm^3}{s} \cdot \frac{1}{mol}\right]$,
- $\dim(\alpha_1) = \left[\frac{mm^3}{s} \cdot \frac{1}{mol}\right]$,
- $\dim(\beta_2) = \left[\frac{mm^3}{s}\right]$.

3.4 Vessel density

Since the equation for the vessel density from [2] goes to zero when the time goes to infinity we need to change our equation for the vessel density a bit since we are now dealing with an equilibrium value for the vessel density. The new equation becomes

$$\frac{\partial \rho}{\partial t} - \underbrace{\epsilon \frac{\partial^2 \rho}{\partial x^2}}_{\substack{\text{random} \\ \text{walk}}} + \gamma(\rho - \rho_{eq}) = \underbrace{\mu_1 \frac{\partial n}{\partial x} - \chi_2 n \frac{\partial c}{\partial x}}_{\text{snail trail}}, \tag{3.4.1}$$

with diffusion coefficient ϵ, increasing or decreasing coefficient γ due to branching and forming loops. Further, we also have coefficient μ_1 which represents the influence of a change in the capillary tip density and coefficient χ_2 which deschribes the influence of the number of tips due to a change in the concentration TG-beta.
Initially there are no vessels present in the damaged part of the heart and there is an equilibrium vessel density around the wound. Far away from the wound the vessel density

should have its equilibrium value and in the center we have a Neumann condition. So we have

$$\rho(x,0) = \begin{cases} 0, & x \in \Omega_w, \\ \rho_{eq}, & x \in \Omega \backslash \Omega_w, \end{cases} \tag{3.4.2}$$

$$\frac{\partial \rho}{\partial x}(0,t) = 0, \quad \rho(1,t) = \rho_{eq}. \tag{3.4.3}$$

Where the dimensions of the coefficients are

- $\dim(\epsilon) = \left[\frac{mm^2}{s}\right]$,
- $\dim(\gamma) = \left[\frac{1}{s}\right]$,
- $\dim(\mu_1) = \left[\frac{mm}{s}\right]$,
- $\dim(\chi_2) = \left[\frac{mm^3}{s} \cdot \frac{mm}{mol}\right]$.

3.5 An alternative model

The model just described is not the only available model we observe. We have a second, more compact, model. This model, based on a model of Maggelakis [5] [6], consists of the following three equations:

$$\frac{\partial m}{\partial t} = -\beta m, \tag{3.5.1}$$

$$\frac{\partial c}{\partial x} - D_1 \frac{\partial^2 c}{\partial x^2} = \alpha m - \lambda c, \tag{3.5.2}$$

$$\frac{\partial n}{\partial t} + \frac{\partial}{\partial x}\left(\chi n \frac{\partial c}{\partial x}\right) = \lambda_2 c(1-n)n, \tag{3.5.3}$$

where the initial and boundary conditions are given by

$$m(x,0) = m_0, \tag{3.5.4}$$

$$c(x,0) = 0, \tag{3.5.5}$$

$$n(x,0) = \begin{cases} 0, & x \in \Omega_w, \\ n_{eq}, & x \in \Omega \backslash \Omega_w, \end{cases} \tag{3.5.6}$$

$$\frac{\partial c}{\partial x}(0,t) = \frac{\partial c}{\partial x}(1,t) = 0, \tag{3.5.7}$$

$$\frac{\partial n}{\partial x}(0,t) = \frac{\partial n}{\partial x}(1,t) = 0. \tag{3.5.8}$$

The equation for the stem cell density, see Equation (3.5.1), is equal to the equation for the stem cell density in our other model, given by (3.1.1). This also holds for the

equation for the concentration TG-beta, see Equation (3.5.2), which is equal to Equation (3.2.1).
The large difference is that no influence is included from the vessel density, in this model we only look at the capillary tip density. An other significant difference is that there is no diffusion, random walk, for the tips included in the alternative model. Hence this alternative model is a simplification of the first model.

The dimensions of the coefficients are

- $\dim(\beta) = \left[\frac{1}{s} \cdot mm^3\right]$,
- $\dim(D_c) = \left[\frac{mm^2}{s}\right]$,
- $\dim(\lambda) = \left[\frac{mol}{s}\right]$,
- $\dim(\lambda_1) = \left[\frac{1}{s}\right]$,
- $\dim(\chi) = \left[\frac{mm^2}{s} \cdot mm^3\right]$,
- $\dim(\lambda_2) = \left[\frac{mm^3}{s} \cdot \frac{mm^3}{mol}\right]$,
- $\dim(1) = \left[\frac{1}{mm^3}\right]$.

Chapter 4

Analytical solutions

In this chapter we determine the analytical solutions to both models. In order to do so, we will neglect terms with insignificant contributions. With help of the analytical solution for the capillary tip density, we find an equation which describes the location of the front of the capillary tips at all times. With this equation we can determine when the front enters the wound, so when vessels are growing into the damaged part of the heart. But first, we determine the analytical solutions to the other equations.

4.1 First model

4.1.1 Stem cell density

The exact solution to Equation (3.1.1) is given by

$$m(x,t) = \begin{cases} m_0 e^{-\beta_1 t}, & x \in \Omega_w, \\ 0, & x \in \Omega \backslash \Omega_w. \end{cases} \tag{4.1.1}$$

4.1.2 Concentration TG-beta

Equation (3.2.1) reflects the evolution of the concentration TG-beta. This equation is used in both models so we use the analytical solution in both models. For this analytical solution we use the domain $\Omega = [0,1]$ where the damaged part of the heart is $\Omega_w = [0,\delta]$. Hence δ is the boundary of the damaged part of the wound.

Since the diffusion of TG-beta is a relatively fast process, we substitute $\frac{\partial}{\partial t} = 0$ into Equation (3.2.1). Using the solution (4.1.1), our problem reduces to

$$-D_1 \frac{\partial^2 c}{\partial x^2} + \lambda c = \alpha m_0 e^{-\beta_1 t} \left(1 - H(x-\delta)\right) \tag{4.1.2}$$

with initial condition (3.2.2), boundary conditions (3.2.3) and where $H(x-\delta)$ is the Heaviside function

$$H(x-\delta) = \begin{cases} 0 & x < \delta, \\ 1 & x \geq \delta. \end{cases}$$

First we determine the homogeneous solution, c_h, of Equation (4.1.2). To this extent we substitute $c_h = e^{rx}$ into Equation (4.1.2) to obtain

$$-D_1 r^2 + \lambda = 0 \quad \Rightarrow \quad r^2 = \frac{\lambda}{D_1} \geq 0 \quad \Rightarrow \quad r = \pm\sqrt{\frac{\lambda}{D_1}},$$

where we substitute $\tilde{\lambda} = \frac{\lambda}{D_1}$ to get

$$c_h(x,t) = A_1 \cosh\left(\sqrt{\tilde{\lambda}}x\right) + A_2 \sinh\left(\sqrt{\tilde{\lambda}}x\right), \qquad \forall x \in [0,\delta), \tag{4.1.3}$$

$$c_h(x,t) = B_1 \cosh\left(\sqrt{\tilde{\lambda}}x\right) + B_2 \sinh\left(\sqrt{\tilde{\lambda}}x\right), \qquad \forall x \in [\delta,1]. \tag{4.1.4}$$

It is easy to see that the particular solution to our nonhomogeneous problem is

$$c_p(x,t) = \frac{\alpha m_0}{\lambda} e^{-\beta 1_t}, \qquad \forall x \in [0,\delta), \tag{4.1.5}$$

$$c_p(x,t) = 0, \qquad \forall x \in [\delta,1]. \tag{4.1.6}$$

Combining (4.1.3)-(4.1.6) we obtain

$$c(x,t) = \frac{\alpha m_0}{\lambda} e^{-\beta 1_t} + A_1 \cosh\left(\sqrt{\tilde{\lambda}}x\right) + A_2 \sinh\left(\sqrt{\tilde{\lambda}}x\right), \qquad \forall x \in [0,\delta), \tag{4.1.7}$$

$$c(x,t) = B_1 \cosh\left(\sqrt{\tilde{\lambda}}x\right) + B_2 \sinh\left(\sqrt{\tilde{\lambda}}x\right), \qquad \forall x \in [\delta,1]. \tag{4.1.8}$$

Further we require that there is continuity on the boundary, $x = \delta$, for both $c(x,t)$ as the derivatives $\frac{\partial c}{\partial x}$. Therefore we obtain

$$\frac{\alpha m_0}{\lambda} e^{-\beta 1_t} + A_1 \cosh\left(\sqrt{\tilde{\lambda}}\delta\right) + A_2 \sinh\left(\sqrt{\tilde{\lambda}}\delta\right) = B_1 \cosh\left(\sqrt{\tilde{\lambda}}\delta\right) + B_2 \sinh\left(\sqrt{\tilde{\lambda}}\delta\right), \tag{4.1.9}$$

$$\sqrt{\tilde{\lambda}}\left(A_1 \sinh\left(\sqrt{\tilde{\lambda}}\delta\right) + A_2 \cosh\left(\sqrt{\tilde{\lambda}}\delta\right)\right) = \sqrt{\tilde{\lambda}}\left(B_1 \sinh\left(\sqrt{\tilde{\lambda}}\delta\right) + B_2 \cosh\left(\sqrt{\tilde{\lambda}}\delta\right)\right). \tag{4.1.10}$$

Using the boundary conditions (bound) and the equalities (4.1.9) and (4.1.10), our analytical solution for the concentration TG-beta is given by (4.1.7) and (4.1.8) with

$$A_1 = -\frac{\alpha m_0}{\lambda} e^{-\beta_1 t} \frac{\sinh\left(\sqrt{\tilde{\lambda}}(1-\delta)\right)}{\sinh\left(\sqrt{\tilde{\lambda}}\right)}, \tag{4.1.11}$$

$$A_2 = 0, \tag{4.1.12}$$

$$B_1 = \frac{\alpha m_0}{\lambda} e^{-\beta_1 t} \frac{\sinh\left(\sqrt{\tilde{\lambda}}\delta\right)}{\tanh\left(\sqrt{\tilde{\lambda}}\right)}, \tag{4.1.13}$$

$$B_2 = -\frac{\alpha m_0}{\lambda} e^{-\beta_1 t} \sinh\left(\sqrt{\tilde{\lambda}}\delta\right). \tag{4.1.14}$$

After a very long time, when there are no stem cells left in the wound, the concentration TG-beta inside the wound goes to

$$t \to \infty \;\Rightarrow\; e^{-\beta_1 t} \to 0 \;\Rightarrow\; c(x,t) \to 0, \tag{4.1.15}$$

and outside the wound it goes directly to

$$t \to \infty \;\Rightarrow\; c(x,t) \to 0. \tag{4.1.16}$$

4.1.3 Amount of TG-beta

In the previous chapter we determined analytically the concentration of TG-beta. It is also possible to determine the number of moles of TG-beta since the number of moles is the concentration integrated over the domain. Taking the integral of Equation (3.2.1) we obtain

$$\frac{d}{dt}\int_\Omega c \; d\Omega - D_1 \int_\Omega \frac{\partial^2 c}{\partial x^2} \; d\Omega + \lambda \int_\Omega c \; d\Omega = \alpha \int_{\Omega_w} m_0 e^{-\beta_1 t} \; d\Omega. \tag{4.1.17}$$

Since we have

$$D_1 \int_\Omega \frac{\partial^2 c}{\partial x^2} \; d\Omega = \left.\frac{\partial c}{\partial x}\right|_0^1 = 0,$$

due to our boundary conditions, Equation (4.1.17) simplifies to

$$\frac{d}{dt}\int_\Omega c \; d\Omega + \lambda \int_\Omega c \; d\Omega = \alpha \int_{\Omega_w} m_0 e^{-\beta_1 t} \; d\Omega. \tag{4.1.18}$$

Substituting $R(t) = \int_\Omega c \; d\Omega$ and using $\Omega_w = [0, \delta)$, Equation (4.1.18) becomes

$$\frac{dR}{dt} + \lambda R = \alpha m_0 e^{-\beta_1 t}(\delta - 0). \tag{4.1.19}$$

Multiplying (4.1.19) with $e^{\lambda t}$ and using

$$e^{\lambda t}\frac{dR}{dt} + \lambda e^{\lambda t} R = \frac{d}{dt}(e^{\lambda t} R),$$

we obtain

$$\frac{d}{dt}(e^{\lambda t} R) = \alpha m_0 e^{(\lambda - \beta_1)t}\delta, \tag{4.1.20}$$

which we integrate to find for $\lambda \neq \beta_1$:

$$\begin{aligned} R(t) =& R_0 e^{-\lambda t} + \frac{\alpha m_0}{\lambda - \beta_1} e^{-\lambda t}(e^{(\lambda-\beta_1)t} - 1)\delta, \\ =& R_0 e^{-\lambda t} + \frac{\alpha m_0}{\lambda - \beta_1}(e^{-\beta_) t} - e^{-\lambda t})\delta, \end{aligned} \tag{4.1.21}$$

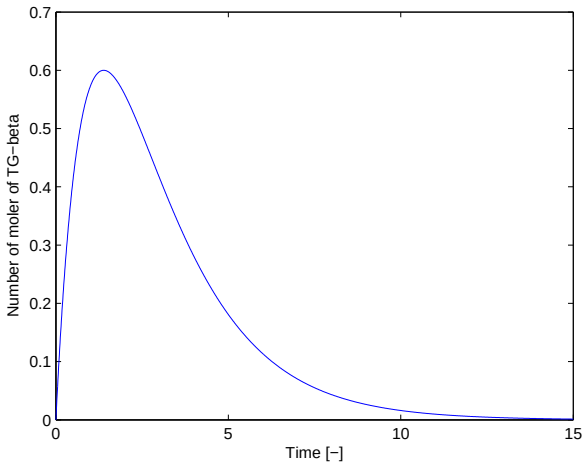

Figure 4.1.1: *Number of moles of TG-beta.*

and for $\lambda = \beta_1$:

$$\begin{aligned} R(t) =& R_0 e^{-\lambda t} + \alpha m_0 \delta e^{-\lambda t} \int_0^t e^0 \, ds, \\ =& R_0 e^{-\lambda t} + \alpha m_0 \delta e^{-\lambda t}. \end{aligned} \tag{4.1.22}$$

In Figure 4.1.1 the number of moles of TG-beta is shown for every time t. Initially there is no TG-beta present and as long as there are stem cells TG-beta is being produced. In Figure 5.4.1 the amount of stem cells is shown. From that figure we conclude that TG-beta is still being produced at $t = 10$, but that the number of moles of TG-beta is decreasing. This means that from a certain moment TG-beta reduces faster than it is being produced.

4.1.4 Vessel density

The equation for the vessel density is given in Equation (3.4.1). In order to find the analytical solution for the vessel density, we use $\frac{\partial}{\partial t} = 0$ again. In Table 5.4.1 we saw that μ_1 is very small, so we neglect the corresponding term. We further have very little influence from diffusion, therefore diffusion is neglected in the analytical solution. By neglecting diffusion, the boundary condition $\frac{\partial \rho}{\partial x}(0, t) = 0$ is no longer necessary. Hence

we have to find the analytical solution to the following problem:

$$\gamma\rho = \gamma\rho_{eq} - \chi_2 n\frac{\partial c}{\partial x}, \tag{4.1.23}$$

$$\rho(x,0) = \begin{cases} 0 & x < \delta, \\ \rho_{eq} & x \geq \delta, \end{cases} \tag{4.1.24}$$

$$\rho(1,t) = \rho_{eq}. \tag{4.1.25}$$

The exact solution is found by combining (4.1.23) with (4.1.24). It is equal to

$$\rho(x,t) = \rho_{eq}H(x-\delta) - \frac{\chi_2}{\gamma}n(x,t)\frac{\partial c}{\partial x}. \tag{4.1.26}$$

This solution also satisfies the boundary condition (4.1.25) since

$$\rho(1,t) = \rho_{eq} - \frac{\chi_2}{\gamma}n(x,t)\frac{\partial c}{\partial x}(1,t) = \rho_{eq}.$$

We have seen in Equation (4.1.15) and Equation (4.1.16) that the concentration of the growth factor TG-beta tends to zero when there are no stem cells left. Therefore the derivative of the concentration TG-beta tends to zero en and becausse of that the vessel density leads to

$$t \to \infty \;\Rightarrow\; \rho(x,t) \to \rho_{eq} \;\forall x \in [0,1]. \tag{4.1.27}$$

So eventually, after the stem cell injection, there is also an equilibrium of vessels inside the wound.

4.1.5 Capillary tip density

The analytical solution for the density of the capillary tips, given by Equation (3.3.1) is difficult to find. First we simplify the problem to

$$\frac{\partial n}{\partial t} + \chi_1\frac{\partial}{\partial x}\left(n\frac{\partial c}{\partial x}\right) = \alpha_0\rho c + \alpha_1 H(c-\hat{c})nc - \beta_2 n\rho, \tag{4.1.28}$$

where we neglect the diffusion part since in reality the problem is dominated by convection. Application of the Product Rule for differentiation

$$\chi_1\frac{\partial}{\partial x}\left(n\frac{\partial c}{\partial x}\right) = \chi_1 n\frac{\partial^2 c}{\partial x^2} + \chi_1\frac{\partial n}{\partial x}\frac{\partial c}{\partial x}.$$

into (4.1.28), gives

$$\frac{dn}{dt} = -\chi_1 n\frac{\partial^2 c}{\partial x^2} + \alpha_0\rho c + \alpha_1 H(c-\hat{c})nc - \beta_2 n\rho = F(n,c), \tag{4.1.29}$$

over a characteristic that travels at speed

$$\frac{dx}{dt} = \chi_1 \frac{\partial c}{\partial x}, \tag{4.1.30}$$

where

$$\frac{dn}{dt} = \frac{\partial n}{\partial t} + \frac{\partial n}{\partial x}\frac{dx}{dt}.$$

Equation (4.1.29) can be rewritten into

$$\frac{dn}{dt} = \left(-\chi_1 \frac{\partial^2 c}{\partial x^2} + \alpha_1 H(c-\hat{c})c - \beta_2 \rho\right) n + \alpha_0 \rho c,$$

where we can use (4.1.26), (4.1.7) and (4.1.8) in order to find the analytical solution.

4.1.6 Characteristics of the capillary tips

For now we focus on the equation for the location of the front of the capillary tips. We define $t = \tau$ as the time that the front is on the boundary of the wound. So $x(\tau) = \delta$. First we determine the location of the front as $x_0 < \delta$ and therefore $t > \tau$. In order to do this, we use (4.1.7), (4.1.11) and (4.1.12).

$$\begin{aligned}
\frac{dx}{dt} =& \chi_1 \frac{\partial c}{\partial x} \\
=& \chi_1 \sqrt{\tilde{\lambda}} \left[A_1 \sinh\left(\sqrt{\tilde{\lambda}}x\right) + A_2 \cosh\left(\sqrt{\tilde{\lambda}}x\right)\right], \\
=& -\frac{\alpha m_0}{\lambda} \chi_1 \sqrt{\tilde{\lambda}} e^{-\beta_1 t} \frac{\sinh\left(\sqrt{\tilde{\lambda}}(1-\delta)\right)}{\sinh\left(\sqrt{\tilde{\lambda}}\right)} \sinh\left(\sqrt{\tilde{\lambda}}x\right).
\end{aligned}$$

Using Seperation of Variables this reduces to

$$\int_{x_0}^{x} \frac{1}{\sinh\left(\sqrt{\tilde{\lambda}}\bar{x}\right)}\, d\bar{x} = -\frac{\alpha m_0}{\lambda} \chi_1 \sqrt{\tilde{\lambda}} \frac{\sinh\left(\sqrt{\tilde{\lambda}}(1-\delta)\right)}{\sinh\left(\sqrt{\tilde{\lambda}}\right)} \int_{\tau}^{t} e^{-\beta_1 \bar{t}}\, d\bar{t}.$$

Using Appendix A.1 on the left hand side the solution is given as

$$\frac{1}{\sqrt{\tilde{\lambda}}} \ln\left(\tanh\left(\frac{\sqrt{\tilde{\lambda}}x}{2}\right)\right)\Bigg|_{x_0}^{x} = \frac{\alpha m_0}{\lambda \beta_1} \chi_1 \sqrt{\tilde{\lambda}} \frac{\sinh\left(\sqrt{\tilde{\lambda}}(1-\delta)\right)}{\sinh\left(\sqrt{\tilde{\lambda}}\right)} (e^{-\beta_1 t} - e^{-\beta_1 \tau}),$$

such that

$$x(t) = \frac{2}{\sqrt{\tilde{\lambda}}}\operatorname{arctanh}\left[\tanh\left(\frac{\sqrt{\tilde{\lambda}}x_0}{2}\right) \cdot \exp\left(\frac{\alpha m_0}{\lambda\beta_1}\chi_1\tilde{\lambda}\frac{\sinh\left(\sqrt{\tilde{\lambda}}(1-\delta)\right)}{\sinh\left(\sqrt{\tilde{\lambda}}\right)}(e^{-\beta_1 t} - e^{-\beta_1\tau})\right)\right], \tag{4.1.31}$$

for $x_0 < \delta$, $t > \tau$.

We can do the same when $x_0 \geq \delta$ and therefore $t \leq \tau$ when using (4.1.8), (4.1.13) and (4.1.14).

$$\begin{aligned}
\frac{dx}{dt} =& \chi_1\frac{\partial c}{\partial x} \\
=& \chi_1\sqrt{\tilde{\lambda}}\left[B_1\sinh\left(\sqrt{\tilde{\lambda}}x\right) + B_2\cosh\left(\sqrt{\tilde{\lambda}}x\right)\right], \\
=& \chi_1\sqrt{\tilde{\lambda}}B_2\left[\cosh\left(\sqrt{\tilde{\lambda}}x\right) - \frac{\sinh\left(\sqrt{\tilde{\lambda}}x\right)}{\tanh\left(\sqrt{\tilde{\lambda}}\right)}\right], \\
=& -\frac{\alpha m_0}{\lambda}\chi_1\sqrt{\tilde{\lambda}}\sinh\left(\sqrt{\tilde{\lambda}}\delta\right)e^{-\beta_1 t}\left[\cosh\left(\sqrt{\tilde{\lambda}}x\right) - \frac{\sinh\left(\sqrt{\tilde{\lambda}}x\right)}{\tanh\left(\sqrt{\tilde{\lambda}}\right)}\right].
\end{aligned}$$

Using Seperation of Variables this reduces to

$$\int_{x_0}^{x}\frac{1}{\cosh\left(\sqrt{\tilde{\lambda}}x\right) - \frac{\sinh\left(\sqrt{\tilde{\lambda}}\bar{x}\right)}{\tanh\left(\sqrt{\tilde{\lambda}}\right)}}\,d\bar{x} = -\frac{\alpha m_0}{\lambda}\chi_1\sqrt{\tilde{\lambda}}\sinh\left(\sqrt{\tilde{\lambda}}\delta\right)\int_0^t e^{-\beta_1\bar{t}}\,d\bar{t}.$$

Substituting

$$\begin{aligned}
A &= \frac{-1}{\tanh\left(\sqrt{\tilde{\lambda}}\right)}, \\
B &= -1,
\end{aligned}$$

and using Appendix A.1 on the left hand side the solution is given as

$$\frac{-1}{\sqrt{\tilde{\lambda}}}\frac{1}{\sqrt{A^2-B^2}}\ln\left(\frac{e^{\sqrt{\tilde{\lambda}}\bar{x}} - \sqrt{\frac{A+B}{A-B}}}{e^{\sqrt{\tilde{\lambda}}\bar{x}} + \sqrt{\frac{A+B}{A-B}}}\right)\Bigg|_{x_0}^{x} = \underbrace{\frac{\alpha m_0}{\lambda\beta_1}\chi_1\sqrt{\tilde{\lambda}}\sinh\left(\sqrt{\tilde{\lambda}}\delta\right)\left(e^{-\beta_1 t} - 1\right)}_{\psi_1(t)}, \tag{4.1.32}$$

such that

$$\frac{e^{\sqrt{\tilde{\lambda}}x}-\sqrt{\frac{A+B}{A-B}}}{e^{\sqrt{\tilde{\lambda}}x}+\sqrt{\frac{A+B}{A-B}}} = \underbrace{\exp\left[\ln\left(\frac{e^{\sqrt{\tilde{\lambda}}x_0}-\sqrt{\frac{A+B}{A-B}}}{e^{\sqrt{\tilde{\lambda}}x_0}+\sqrt{\frac{A+B}{A-B}}}\right)-\sqrt{\tilde{\lambda}}\sqrt{A^2-B^2}\psi_1(t)\right]}_{\psi_2(t)},$$

$$\Rightarrow\ x(t)=\frac{1}{\sqrt{\tilde{\lambda}}}\ln\left(\sqrt{\frac{A+B}{A-B}}\cdot\frac{1+\psi_2(t)}{1-\psi_2(t)}\right), \tag{4.1.33}$$

for $x_0 \geq \delta$, $t \leq \tau$.

Note that if $x_0 < \delta$, the front has already passed the boundary of the wound and we immediately have $\tau = 0$. If $x_0 \geq \delta$, τ can be determined from (4.1.32) with substituting $x(\tau) = \delta$.

In Figure 4.1.2(a) the movement of the characteristics of the capillary tip density is shown for the situation that the characteristics already start in the wound of the heart. In this figure we see that the speed of the characteristics decreases as the characteristics move towards the center of the wound. Note that this is the conclusion in this situation with a certain choice for all the biological parameters.

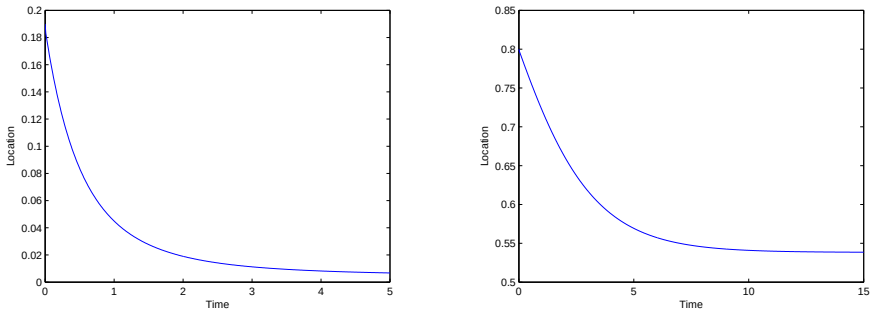

(a) Characteristics start inside the wound at $x = 0.19$

(b) Characteristics start outside the wound at $x = 0.8$

Figure 4.1.2: *The movement of the characteristics of the capillary tip density.*

In Figure 4.1.2(b) the movement is shown for the characteristics of the capillary tips when they are initially outside the wound. When the characteristics reach δ, the boundary of the wound, the characteristics follow equation (4.1.31) instead of (4.1.33). Here we have $\delta = 0.2$. For the chosen values of our parameters we see that the characteristics never reach the boundary of the heart. The characteristics move through $\frac{dx}{dt} = \chi_1 \frac{\partial c}{\partial x}$, where χ_1 is a biological constant parameter. This means that $\frac{\partial c}{\partial x}$ goes to zero before the front can reach the boundary of the wound. The only parameter that is not fixed by biology, is the amount of injected stem cells. So from Figure 4.1.2(b) we conclude that not enough stem cells are injected here in order to have an improvement of the density of capillary tips inside the heart.

4.2 An alternative model

The equations for the the stem cell density and the concentration TG-beta are the same as in the first model. Therefore, the exact solutions are given by (4.1.1), (4.1.7) and (4.1.8). Only the analytically solution for Equation (3.5.3), with initial condition (3.5.6) and boundary conditions (3.5.8), need to be determined.

For the derivative of the capillary tip density with respect to time t we obtain

$$\frac{dn}{dt} = \frac{\partial n}{\partial t} + \frac{\partial n}{\partial x}\frac{dx}{dt} \equiv F(n, c), \tag{4.2.1}$$

where $F(n, c)$ represent the characteristics.

Rewriting Equation (3.5.3) we get

$$\frac{\partial n}{\partial t} + \chi \frac{\partial c}{\partial x}\frac{\partial n}{\partial x} = -\chi \frac{\partial^2 c}{\partial x^2} n + \lambda_2 c(1-n)n. \tag{4.2.2}$$

Combining Equation (4.2.1) and Equation (4.2.2) we obtain

$$\frac{dn}{dt} = -\chi \frac{\partial^2 c}{\partial x^2} n + \lambda_2 c(1-n)n \equiv F(n, c), \tag{4.2.3}$$

$$\frac{dx}{dt} = \chi \frac{\partial c}{\partial x}. \tag{4.2.4}$$

For the solutions for these equations we need the derivatives of c with respect to x. They can be determined from Equation (4.1.7) and Equation (4.1.8).

For Equation (4.2.3) we have the solution

$$n(t) = n(0) \exp\left(\int_0^t -\chi \frac{\partial^2 c}{\partial x^2}(x(s), s) + \lambda_2 c(x(s), s)\left(1 - n(x(s), s)\right)\ ds \right),$$

over a characteristic. And for Equation (4.2.4) we have

$$x(t) = x_0 + \chi \int_0^t \frac{\partial c}{\partial x}(x(s), s)\ dx. \tag{4.2.5}$$

4.2.1 Characteristics of the capillary tips

In order to find the function for $x(t)$, the characteristics of the capillary tips, we need to split the function into two: One if the characteristics are initially in the damaged part of the wound ($x_0 < \delta$) and one if the characteristics are initially outside the wound ($x_0 \geq \delta$). We assume that at time $t = \tau$ the front of the capillary tips enters the wound.

The solutions to $x(t)$ are the same solutions as in our previous model since $c(x, t)$ has the same solution for both models and therefore $\frac{\partial c}{\partial x}$ has the same solution for both models. Therefore the solutions are given by (4.1.31) and (4.1.33).

Chapter 5

One dimensional finite difference method

To determine the solution for our model we approximate all equations, except the one for the stem cell density, using numerical methods. Since the equation for the stem cell density has been easily solved analytically we use the results contained in (4.1.1).

In this chapter we use the finite difference method where we discretize in both spatial (j) and time (k) direction. We observe the solutions in N points with equal distance Δx.

5.1 Concentration TG-beta

Since Equation (3.2.1) is a linear equation we use the Euler backwards method and a central discretization for the second derivative. This leads to the following discretization:

$$\frac{c_j^{k+1} - c_j^k}{\Delta t} - D_1 \frac{c_{j+1}^{k+1} - 2c_j^{k+1} + c_{j-1}^{k+1}}{(\Delta x)^2} + \lambda c_j^{k+1} = \alpha m_j^{k+1},$$

$$\implies c_j^{k+1} - \Delta t D_1 \frac{c_{j+1}^{k+1} - 2c_j^{k+1} + c_{j-1}^{k+1}}{(\Delta x)^2} + \Delta t \lambda c_j^{k+1} = c_j^k + \Delta t \alpha m_j^{k+1},$$

gives

$$c_{j-1}^{k+1}\left(\frac{-\Delta t D_1}{(\Delta x)^2}\right) + c_j^{k+1}\left(1 + \frac{2\Delta t D_1}{(\Delta x)^2} + \Delta t\lambda\right) + c_{j+1}^{k+1}\left(\frac{-\Delta t D_1}{(\Delta x)^2}\right) = c_j^k + \Delta t \alpha m_j^{k+1}. \tag{5.1.1}$$

With initial condition (3.2.2) and the boundary conditions (3.2.3) such that

$$\frac{c_2 - c_0}{\Delta x} = 0 \Rightarrow \ c_0 = c_2,$$
$$\frac{c_{N+1} - c_{N-1}}{\Delta x} = 0 \Rightarrow \ c_{N+1} = c_{N-1}.$$

Equation (5.1.1) can be solved for each j by

$$(\mathbf{I} + \Delta t \mathbf{A_c})\, \mathbf{c}^{k+1} = (\mathbf{I} + \Delta t \mathbf{A_c}) \left(\mathbf{c}^k + \Delta t \mathbf{b_c} \right), \tag{5.1.2}$$

where $\mathbf{I}$ is the identity matrix and

$$\mathbf{A_c} = \frac{1}{(\Delta x)^2} \begin{pmatrix} 2D_1 + \lambda(\Delta x)^2 & -2D_1 & & & & \\ -D_1 & 2D_1 + \lambda(\Delta x)^2 & -D_1 & & & \emptyset \\ & \ddots & \ddots & \ddots & & \\ & & -D_1 & 2D_1 + \lambda(\Delta x)^2 & -D_1 & \\ \emptyset & & & -2D_1 & 2D_1 + \lambda(\Delta x)^2 & \end{pmatrix}, \tag{5.1.3}$$

and

$$\mathbf{b_c} = \begin{pmatrix} \alpha m_1^{k+1} \\ \vdots \\ \alpha m_j^{k+1} \\ \vdots \\ \alpha m_N^{k+1} \end{pmatrix}. \tag{5.1.4}$$

5.2 Capillary tip density

The equation for the capillary tip density, Equation (3.3.1), is a more complicated equation since it contains the chemotaxis term $\chi_1 \frac{\partial}{\partial x}\left(n \frac{\partial c}{\partial x}\right)$, which acts as a convection term. Again we use the implicit Euler backwards method and a central discretization. Since the term ρ_j^{k+1} depends on the solution of n_j^{k+1} we approximate it explicit. This method, a combination of an implicit and explicit approximation is called IMEX.

$$\frac{n_j^{k+1} - n_j^k}{\Delta t} + \underbrace{\frac{\chi_1}{\Delta x}\left(n_{j+\frac{1}{2}}^{k+1} \frac{c_{j+1}^{k+1} - c_j^{k+1}}{\Delta x} - n_{j-\frac{1}{2}}^{k+1} \frac{n_j^{k+1} - n_{j-1}^{k+1}}{\Delta x} \right)}_{G(n_{j-1/2}, n_{j+1/2}, c_{j-1}, c_j, c_{j+1})} - D_2 \frac{n_{j+1}^{k+1} - 2n_j^{k+1} + n_{j-1}^{k+1}}{(\Delta x)^2}$$
$$= \alpha_0 \rho_j^{k+1} c_j^{k+1} + \alpha_1 H\left(c_j^{k+1} - \hat{c}\right) n_j^{k+1} c_j^{k+1} - \beta_2 n_j^{k+1} \rho_j^{k+1}.$$

The part $G(n_{j-1/2}, n_{j+1/2}, c_{j-1}, c_j, c_{j+1})$ equals

$$\begin{aligned} G(n_{j-1/2}, n_{j+1/2}, c_{j-1}, c_j, c_{j+1}) &= \frac{\chi_1}{\Delta x}\left(n_{j+\frac{1}{2}}^{k+1} \frac{c_{j+1}^{k+1} - c_j^{k+1}}{\Delta x} - n_{j-\frac{1}{2}}^{k+1} \frac{c_j^{k+1} - c_{j-1}^{k+1}}{\Delta x} \right) \\ &= \frac{\chi_1}{\Delta x}\left(\frac{n_j^{k+1} + n_{j+1}^{k+1}}{2} \frac{c_{j+1}^{k+1} - c_j^{k+1}}{\Delta x} - \frac{n_j^{k+1} + n_{j-1}^{k+1}}{2}^{k+1} \frac{c_j^{k+1} - c_{j-1}^{k+1}}{\Delta x} \right) \\ &= \frac{\chi_1}{2(\Delta x)^2}\left(n_{j-1}^{k+1}\left(c_{j-1}^{k+1} - c_j^{k+1}\right) + n_j^{k+1}\left(c_{j+1}^{k+1} - 2c_j^{k+1} + c_{j-1}^{k+1}\right) \right. \\ &\qquad \left. + n_{j+1}^{k+1}\left(c_{j+1}^{k+1} - c_j^{k+1}\right) \right). \end{aligned}$$

Therefore the discretization becomes

$$n_j^{k+1} + \Delta t \left(G - D_2 \frac{n_{j+1}^{k+1} - 2n_j^{k+1} + n_{j-1}^{k+1}}{(\Delta x)^2} \right) = n_j^k + \Delta t \left(\alpha_0 \rho_j^k c_j^{k+1} + \alpha_1 H \left(c_j^{k+1} - \hat{c} \right) n_j^{k+1} c_j^{k+1} - \beta_2 n_j^{k+1} \rho_j^k \right),$$

$$\begin{aligned} \implies & n_{j-1}^{k+1} \left(\frac{-\Delta t D_2}{(\Delta x)^2} + \frac{\chi_1 \Delta t}{2(\Delta x)^2} \left(c_{j-1}^{k+1} - c_j^{k+1} \right) \right) \\ & + n_j^{k+1} \left(1 + \frac{2\Delta t D_2}{(\Delta x^2} + \frac{\chi_1 \Delta t}{2(\Delta x)^2} \left(c_{j+1}^{k+1} - 2c_{j-1}^{k+1} + c_{j-1}^{k+1} \right) - \Delta t \alpha_1 H \left(c_j^{k+1} - \hat{c} \right) c_j^{k+1} \right. \\ & \left. + \Delta t \beta_2 \rho_j^{k+1} \right) + n_{j+1}^{k+1} \left(\frac{-\Delta t D_2}{(\Delta x)^2} + \frac{\chi_1 \Delta t}{2(\Delta x)^2} \left(c_{j+1}^{k+1} - c_j^{k+1} \right) \right) = n_j^k + \Delta t \alpha_0 \rho_j^k c_j^{k+1}. \quad (5.2.1) \end{aligned}$$

With initial condition (3.3.3) and the boundary conditions (3.3.4), we obtain

$$\begin{aligned} \frac{n_2 - n_0}{\Delta x} = 0 \Rightarrow \ n_0 = n_2, \\ \frac{n_{N+1} - n_{N-1}}{\Delta x} = 0 \Rightarrow \ n_{N+1} = n_{N-1}. \end{aligned}$$

Equation (5.2.1) can be solved for each j by

$$\mathbf{n}^{k+1} = (\mathbf{I} + \Delta t \mathbf{A_n})^{-1} \left(\mathbf{n}^k + \Delta t \mathbf{b_n} \right), \quad (5.2.2)$$

where $\mathbf{I}$ is again the identity matrix. Since $\mathbf{A_n}$ has very big entries we only show the nonzero entries of the matrix:

$$\begin{aligned} \mathbf{A_n}_{j,j-1} =& \frac{1}{(\Delta x)^2} \left(-D_2 + \frac{\chi_1}{2} \left(c_{j-1}^{k+1} - c_j^{k+1} \right) \right), \\ \mathbf{A_n}_{j,j} =& \frac{1}{(\Delta x)^2} \left(2D_2 + \frac{\chi_1}{2} \left(c_{j+1}^{k+1} - 2c_j^{k+1} + c_{j-1}^{k+1} \right) - \alpha_1 H \left(c_j^{k+1} - \hat{c} \right) c_j^{k+1} (\Delta x)^2 \right. \\ & \left. + \beta_2 \rho_j^k (\Delta x)^2 \right), \\ \mathbf{A_n}_{j,j+1} =& \frac{1}{(\Delta x)^2} \left(-D_2 + \frac{\chi_1}{2} \left(c_{j+1}^{k+1} - c_j^{k+1} \right) \right), \end{aligned}$$

where we have on the boundaries, due to the boundary conditions (3.2.3), (3.3.4) and

(3.4.3):

$$\begin{aligned}
\mathbf{A_n}_{1,1} =& \frac{1}{(\Delta x)^2}\left(2D_2 + \frac{\chi_1}{2}\left(c_2^{k+1} - 2c_1^{k+1} + c_0^{k+1}\right) - \alpha_1 H\left(c_1^{k+1} - \hat{c}\right)c_1^{k+1}(\Delta x)^2\right. \\
&\left. +\beta_2\rho_1^k(\Delta x)^2\right) \\
=& \frac{1}{(\Delta x)^2}\left(2D_2 + \chi_1\left(c_2^{k+1} - c_1^{k+1}\right) - \alpha_1 H\left(c_1^{k+1} - \hat{c}\right)c_1^{k+1}(\Delta x)^2\right. \\
&\left. +\beta_2\rho_1^k(\Delta x)^2\right), \\
\mathbf{A_n}_{1,2} =& \frac{1}{(\Delta x)^2}\left(-D_2 + \frac{\chi_1}{2}\left(c_2^{k+1} - c_1^{k+1}\right) - D_2 + \frac{\chi_1}{2}\left(c_0^{k+1} - c_1^{k+1}\right)\right) \\
=& \frac{2}{(\Delta x)^2}\left(-D_2 + \frac{\chi_1}{2}\left(c_2 - c_1\right)\right), \\
\mathbf{A_n}_{N,N-1} =& \frac{1}{(\Delta x)^2}\left(-D_2 + \frac{\chi_1}{2}\left(c_{N-1}^{k+1} - c_N^{k+1}\right) - D_2 + \frac{\chi_1}{2}\left(c_{N+1}^{k+1} - c_N^{k+1}\right)\right) \\
=& \frac{2}{(\Delta x)^2}\left(-D_2 + \frac{\chi_1}{2}\left(c_{N-1} - c_N\right)\right), \\
\mathbf{A_n}_{N,N} =& \frac{1}{(\Delta x)^2}\left(2D_2 + \frac{\chi_1}{2}\left(c_{N+1}^{k+1} - 2c_N^{k+1} + c_{N-1}^{k+1}\right) - \alpha_1 H\left(c_N^{k+1} - \hat{c}\right)c_N^{k+1}(\Delta x)^2\right. \\
&\left. +\ \beta_2\rho_N^k(\Delta x)^2\right) \\
=& \frac{1}{(\Delta x)^2}\left(2D_2 + \chi_1\left(c_{N-1}^{k+1} - c_N^{k+1}\right) - \alpha_1 H\left(c_N^{k+1} - \hat{c}\right)c_N^{k+1}(\Delta x)^2\right. \\
&\left. +\beta_2\rho_{eq}^k(\Delta x)^2\right).
\end{aligned}$$

And as last $\mathbf{b_n}$ in equation (5.2.2) equals

$$\mathbf{b_n} = \begin{pmatrix} \alpha_0\rho_1^k c_1^{k+1} \\ \vdots \\ \alpha_0\rho_j^k c_j^{k+1} \\ \vdots \\ \alpha_0\rho_N^k c_N^{k+1} \end{pmatrix}. \tag{5.2.3}$$

5.3 Vessel density

Equation (3.4.1) is again a relatively easy equation so we can just use Euler backwards and a central discretization. The discretization is given by

$$\frac{\rho_j^{k+1} - \rho_j^k}{\Delta t} - \epsilon\frac{\rho_{j+1}^{k+1} - 2\rho_j^{k+1} + \rho_{j-1}^{k+1}}{(\Delta x)^2} + \gamma\rho_j^{k+1} - \gamma\rho_{eq} = \mu_1\frac{n_{j+1}^{k+1} - n_{j-1}^{k+1}}{2\Delta x} - \chi_2 n_j^{k+1}\frac{c_{j+1}^{k+1} - c_{j-1}^{k+1}}{2\Delta x},$$

$$\implies \rho_j^{k+1} + \Delta t \left(-\epsilon \frac{\rho_{j+1}^{k+1} - 2\rho_j^{k+1} + \rho_{j-1}^{k+1}}{(\Delta x)^2} + \gamma \rho_j^{k+1} - \gamma \rho_{eq} \right) = \rho_j^k + \Delta t \left(\mu_1 \frac{n_{j+1}^{k+1} - n_{j-1}^{k+1}}{2\Delta x} - \chi_2 n_j^{k+1} \frac{c_{j+1}^{k+1} - c_{j-1}^{k+1}}{2\Delta x} \right),$$

gives

$$\rho_{j-1}^{k+1} \left(\frac{-\epsilon \Delta t}{(\Delta x)^2} \right) + \rho_j^{k+1} \left(1 + \frac{2\Delta t \epsilon}{(\Delta x)^2} + \Delta t \gamma \right) + \rho_{j+1}^{k+1} \left(\frac{-\epsilon \Delta t}{(\Delta x)^2} \right) = \rho_j^k + \Delta t \left(\mu_1 \frac{n_{j+1}^{k+1} - n_{j-1}^{k+1}}{2\Delta x} - \chi_2 n_j^{k+1} \frac{c_{j+1}^{k+1} - c_{j-1}^{k+1}}{2\Delta x} + \gamma \rho_{eq} \right). \quad (5.3.1)$$

With initial condition (3.4.2) and the boundary conditions (3.4.3) such that

$$\frac{\rho_2 - \rho_0}{\Delta x} = 0 \Rightarrow \ \rho_0 = \rho_2,$$
$$\rho(1,t) = \rho_{eq} \Rightarrow \ \rho_{N+1} = \rho_{eq}.$$

Equation (3.4.1) can now be solved for each j by

$$\rho^{k+1} = (\mathbf{I} + \Delta t \mathbf{A}_\rho)^{-1} \left(\rho^k + \Delta t \mathbf{b}_\rho \right), \quad (5.3.2)$$

where $\mathbf{I}$ is again the identity matrix and

$$\mathbf{A}_\rho = \frac{1}{(\Delta x)^2} \begin{pmatrix} 2\epsilon + \gamma(\Delta x)^2 & -2\epsilon & & & & \\ -\epsilon & 2\epsilon + \gamma(\Delta x)^2 & -\epsilon & & & \emptyset \\ & \ddots & \ddots & \ddots & & \\ & & -\epsilon & 2\epsilon + \gamma(\Delta x)^2 & -\epsilon & \\ \emptyset & & & -\epsilon & 2\epsilon + \gamma(\Delta x)^2 & \end{pmatrix}, \quad (5.3.3)$$

and

$$\mathbf{b_c} = \begin{pmatrix} \mu_1 \frac{n_2^{k+1} - n_0^{k+1}}{2\Delta x} - \chi_2 n_j^{k+1} \frac{c_2^{k+1} - c_0^{k+1}}{2\Delta x} + \gamma \rho_{eq} \\ \vdots \\ \mu_1 \frac{n_{j+1}^{k+1} - n_{j-1}^{k+1}}{2\Delta x} - \chi_2 n_j^{k+1} \frac{c_{j+1}^{k+1} - c_{j-1}^{k+1}}{2\Delta x} + \gamma \rho_{eq} \\ \vdots \\ \mu_1 \frac{n_N^{k+1} - n_{N-2}^{k+1}}{2\Delta x} - \chi_2 n_j^{k+1} \frac{c_N^{k+1} - c_{N-2}^{k+1}}{2\Delta x} + \gamma \rho_{eq} \\ \mu_1 \frac{n_{N+1}^{k+1} - n_{N-1}^{k+1}}{2\Delta x} - \chi_2 n_j^{k+1} \frac{c_{N+1}^{k+1} - c_{N-1}^{k+1}}{2\Delta x} + \gamma \rho_{eq} + \frac{\epsilon}{(\Delta x)^2} \rho_{eq} \end{pmatrix}. \quad (5.3.4)$$

Where $\mathbf{b}_\rho$ equals, due to boundary conditions (3.2.3), (3.3.4) and (3.4.3)

$$\mathbf{b}_\rho = \begin{pmatrix} \gamma\rho_{eq} \\ \mu_1 \frac{n_3^{k+1} - n_1^{k+1}}{2\Delta x} - \chi_2 n_2^{k+1} \frac{c_3^{k+1} - c_1^{k+1}}{2\Delta x} + \gamma\rho_{eq} \\ \vdots \\ \vdots \\ \mu_1 \frac{n_N^{k+1} - n_{N-2}^{k+1}}{2\Delta x} - \chi_2 n_{N-1}^{k+1} \frac{c_N^{k+1} - c_{N-2}^{k+1}}{2\Delta x} + \gamma\rho_{eq} \\ \gamma\rho_{eq} \frac{\epsilon}{(\delta x)^2} \rho_{eq} \end{pmatrix} \tag{5.3.5}$$

5.4 Numerical simulations and parameter values

Before we look at the exact solution for the stem cell density and the approximations for the concertration TG-beta, the capillary tip density and the vessel density we need to define the values of our coefficients for our model and the different step sizes we use for our approximations. The values of our constants are shown in Table 5.5.1.

Name	Value	Description
Ω_w	0.2	Distance to core of the 'wound' in the heart
m_0	2	Initial density of stem cells, in million stem cells
β_1	0.5	Decay of stem cells
D_1	1	Diffusion coefficient for TG-beta
α	3	Growth of TG-beta
λ	1	Decay of TG-beta
χ_1	0.4	Attraction of TG-beta
D_2	1	Diffusion coefficient for the capillary tips
α_0	50	Growth of tip density due to primary angiogenesis
α_1	10	Growth of tipd ensity due to secondary angiogenesis
$\hat{c}$	0.2	Threshold of concentration TG-beta
β_2	50	Decay of tip density due to anastomoses
ϵ	0.01	Diffusion coefficient for vessels
γ	0.25	Decay of blood vessels
ρ_{eq}	0.001	Equilibrium value of vessel density
μ_1	0.001	Growth/decay of vessel density influenced by growth/decay in tip density
χ_2	0.4	Growth/decay of vessel density influenced by the number of tips due to growth/decay in concentration TG-beta

Table 5.4.1: *Values of the coefficients in our model* [2].

As mentioned before we have an exact solution of the density for the stem cells.
In Figure 5.4.1 we see the exact solution of the stem cell density in time. The figure illustrates how the density of stem cells is equal everywhere in the wound of the heart

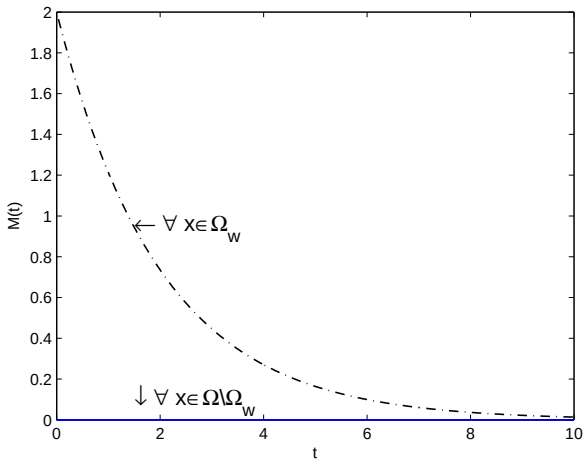

Figure 5.4.1: *The exact solution for the density of stem cells inside and outside the damaged part of the wound.*

at a time t. Further we see that initially the density equals 2 million cells/mm^3 - which is probably not a realistic value, we use this for our mathematical purposes - and that it decreases exponentially in time, so after $t = 2$ the density is around the 0.75 million cells/ mm^3. After there are no stem cells left the 'production' of TG-beta ends and the angiogenesis trigger due to this attractant TG-beta comes to an end. This does not mean that the angiogenesis itself has come to an end.
In Figure 5.4.2 the concentration TG-beta is shown for different times t. Initially there is no TG-beta present. When the stem cells are injected, they 'release' some TG-beta. Since the stem cells are injected in the wound of the heart, Ω_w, the 'production' of TG-beta finds place in Ω_w. From there the attractant TG-beta will spread towards outside Ω_w. Hence at the beginning the most attractant is in Ω_w. After a while the attractant is more spread around the wound. Since the stem cells decrease exponentially, the production of TG-beta will come to an end. This can be seen in Figure 5.4.2 where the concentration attractant is already decreasing in the core of the wound.

In Figure 5.4.3 we see the capillary tip density for different time t. Initially there are no tips. The first tips are formed at the boundary of the wound since that is the first location in time where the attractant meets the vessels. Vessels are constantly branching of and forming new loops such that the tip density increases and decreases. After a while, when the attractant has spread, vessels outside the heart wound also branch of and more tips are formed.
At that moment the amount of stem cells has decreased enormously and no more TG-beta is being produced inside the wound, no more vessels will branch of near the wound and since vessels keep forming new loops, the density of capillary tips will decrease in

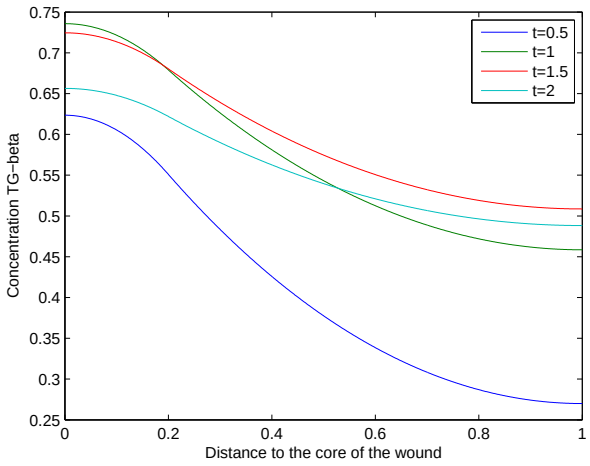

Figure 5.4.2: *Concentration TG-beta with* $\Delta x = 0.001,\ \Delta t = 0.01$ *and* $T = 2$.

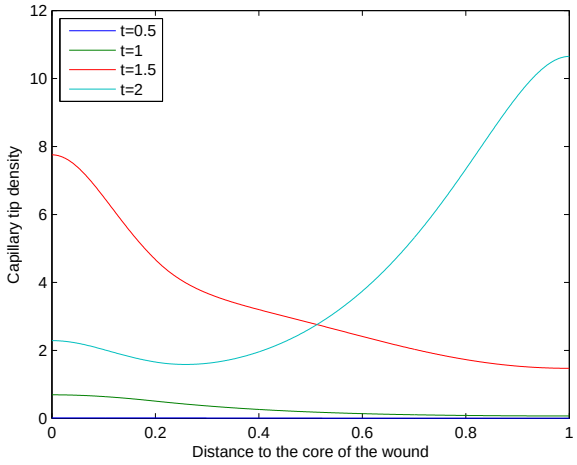

Figure 5.4.3: *Capillary tip density with* $\Delta x = 0.001,\ \Delta t = 0.01$ *and* $T = 2$.

and near the wound. As long as some TG-beta is still present far away from the wound the tip density keeps increasing there for a while. So there is a time interval during which the density of capillary tips is decreasing inside and near the wound and at the same time, it is increasing further away from the wound. This can be seen in 5.4.3 at $t = 2$.

Combined with the change in the capillary tip density, the vessel density changes since both densities are influenced by each other.

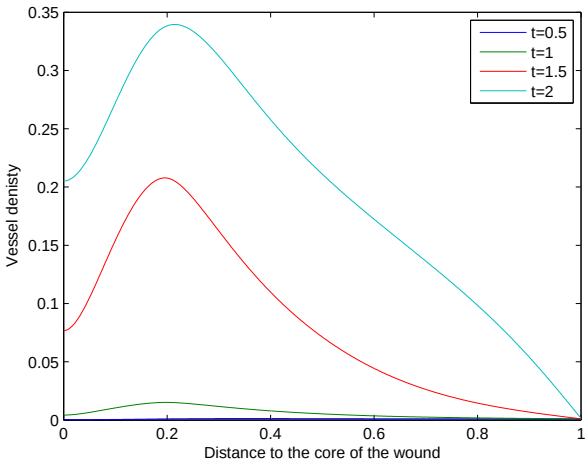

Figure 5.4.4: *Vessel density with* $\Delta x = 0.001,\ \Delta t = 0.01$ *and* $T = 2$.

Initially the vessel density has an equilibrium value, $\rho_{eq} = 0.001$, outside the wound and it was zero inside the wound. This can still be deduced from Figure 5.4.4 at $t = 0.5$. Due to the increasing concentration TG-beta a few vessels are grown into the wound of the heart after a short time. The growth of the vessel density is maximal around the wound since the concentration TG-beta is much higher here than far away from the wound. This is shown in Figure 5.4.4 at $t = 1$. Further, since initially there were no vessels in the wound, however there were vessels at the surface of the wound, we see at all times that the vessel density is highest around the surface of the wound. And as we can see in all figures, there is always just a little bit of attractant present far away from the wound such that there is not much branching over there.

Since the stem cells are decreasing exponentially there are no stem cells left after a long time. Therefore the 'production' of the concentration TG-beta will stop eventually. We wonder how this effects the capillary tip density and the vessel density in the long term. This is shown in Figure 5.4.5.

In Figure 5.4.5(a) we see that due to the decreasing stem cells the concentration TG-beta will indeed tend to zero as time increases. Without this attractant the capillary tip density will also go to zero and no new tips will be formed anymore, this is shown in Figure 5.4.5(b). Due to the concentration TG-beta that decreases and the tip density that goes to zero vessels will not branch off anymore and vessels will no longer form any loops. Therefore, as we can see in Figure 5.4.5(c) and 5.4.5(d) the vessel density will go to its initial value, the equilibrium value of ρ_{eq}.

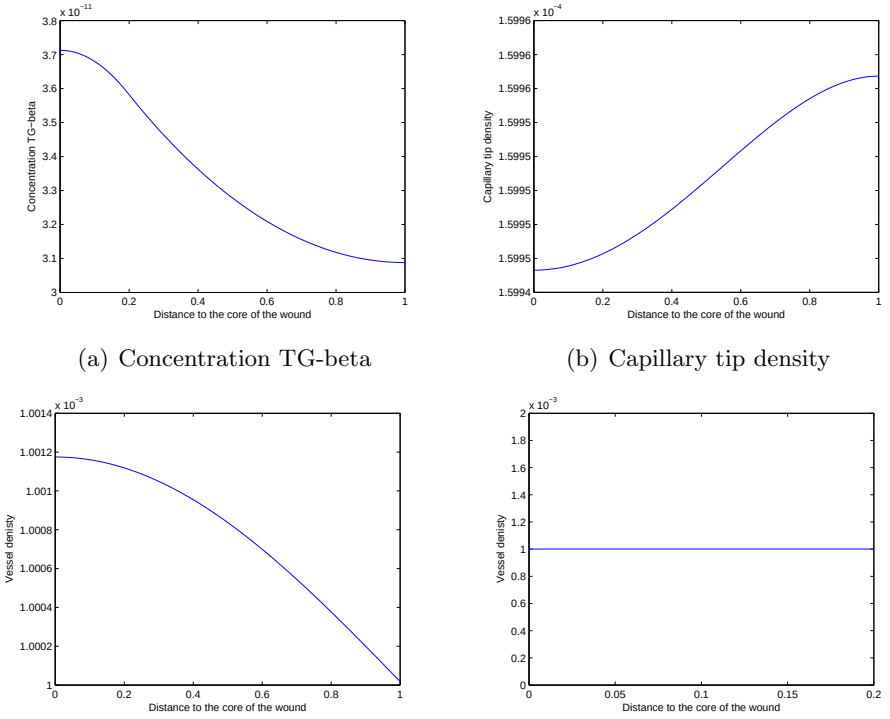

(a) Concentration TG-beta

(b) Capillary tip density

(c) Vessel density

(d) Vessel density in the wound

Figure 5.4.5: *Values after* $T = 50$ *with* $\Delta x = 0.01$ *and* $\Delta t = 0.1$.

In Chapter 4 we have shown analytically that the the concentration TG-beta, and the vessel density converges respectively to zero and ρ_{eq}.

Before an injection of stem cells there were no vessels inside the wound. From Figure 5.4.5(d) we conclude that after the stem cells are reduced to zero the vessel density inside the wound has an equilibrium value different than zero.

5.5 Alternative model

In Chapter 3 we have introduced an alternative model. Since the equation for the concentration TG-beta is the same as in the first model the discretization will be the same as discussed in Chapter 5.1. Of course the exact solution for the stem cell density, given by (4.1.1), will be used.

Now we only need to discretize Equation (3.5.3). Using the implicit Euler backwards

method and a Picard iteration for the nonlinear term the discretization becomes

$$\frac{n_j^{k+1}-n_j^k}{\Delta t}+\underbrace{\frac{\chi}{\Delta x}\left(n_{j+\frac{1}{2}}^{k+1}\frac{c_{j+1}^{k+1}-c_j^{k+1}}{\Delta x}-n_{j-\frac{1}{2}}^{k+1}\frac{c_j^{k+1}-c_{j-1}^{k+1}}{\Delta x}\right)}_{G(n_{j-1/2},n_{j+1/2},c_{j-1},c_j,c_{j+1})}=\lambda_2 c_j^{k+1}(1-n_j^{k+1})n_j^{k+1},$$

where we see that we need $(n_j^{k+1})^2$. Since this term depends on the solution of n_j^{k+1} we approximate this in an explicit way. So the term $\lambda_2 c_j^{k+1}(1-n_j^{k+1})n_j^{k+1}$ will be approximated by $\lambda_2 c_j^{k+1}(1-n_j^k)n_j^{k+1}$. Therefore we actually use the IMEX method.

The part $G(n_{j-1/2},n_{j+1/2},c_{j-1},c_j,c_{j+1})$ equals

$$\begin{aligned}
G(n_{j-1/2},n_{j+1/2},c_{j-1},c_j,c_{j+1}) &= \frac{\chi_1}{\Delta x}\left(n_{j+\frac{1}{2}}^{k+1}\frac{c_{j+1}^{k+1}-c_j^{k+1}}{\Delta x}-n_{j-\frac{1}{2}}^{k+1}\frac{c_j^{k+1}-c_{j-1}^{k+1}}{\Delta x}\right)\\
&= \frac{\chi_1}{\Delta x}\left(\frac{n_j^{k+1}+n_{j+1}^{k+1}}{2}\frac{c_{j+1}^{k+1}-c_j^{k+1}}{\Delta x}-\frac{n_j^{k+1}+n_{j-1}^{k+1}}{2}{}^{k+1}\frac{c_j^{k+1}-c_{j-1}^{k+1}}{\Delta x}\right)\\
&= \frac{\chi_1}{2(\Delta x)^2}\left(n_{j-1}^{k+1}\left(c_{j-1}^{k+1}-c_j^{k+1}\right)+n_j^{k+1}\left(c_{j+1}^{k+1}-2c_j^{k+1}+c_{j-1}^{k+1}\right)\right.\\
&\qquad \left.+n_{j+1}^{k+1}\left(c_{j+1}^{k+1}-c_j^{k+1}\right)\right).
\end{aligned}$$

Therefore the discretization becomes

$$\begin{aligned}
&\implies n_{j-1}^{k+1}\left(\frac{\chi\Delta t}{2(\Delta x)^2}\left(c_{j-1}^{k+1}-c_j^{k+1}\right)\right)\\
&+n_j^{k+1}\left(1+\frac{\chi\Delta t}{2(\Delta x)^2}\left(c_{j+1}^{k+1}-2c_{j-1}^{k+1}+c_{j-1}^{k+1}\right)c_j^{k+1}(1-n_j^{k+1})n_j^{k+1}-\Delta t\lambda_2 c_j^{k+1}\left(1-n_j^k\right)\right)\\
&+n_{j+1}^{k+1}\left(\frac{\chi\Delta t}{2(\Delta x)^2}\left(c_{j+1}^{k+1}-c_j^{k+1}\right)\right)=n_j^k. \qquad (5.5.1)
\end{aligned}$$

With initial condition (3.5.6) and the boundary conditions (3.5.8) which we discretize in a central way such that

$$\begin{aligned}
\frac{n_2-n_0}{\Delta x}=0 \Rightarrow\ n_0=n_2,\\
\frac{n_{N+1}-n_{N-1}}{\Delta x}=0 \Rightarrow\ n_{N+1}=n_{N-1}.
\end{aligned}$$

Equation (5.5.1) can be solved for each j by

$$\mathbf{n}^{k+1}=(\mathbf{I}+\Delta t\mathbf{A_n})^{-1}\left(\mathbf{n}^k+\Delta t\mathbf{b_n}\right), \qquad (5.5.2)$$

where $\mathbf{I}$ is again the identity matrix. Since $\mathbf{A_n}$ has very large entries we only show the nonzero entries of the matrix:

$$\begin{aligned}
\mathbf{A_n}_{j,j-1} =& \frac{\chi}{2(\Delta x)^2}\left(c_{j-1}^{k+1} - c_j^{k+1}\right), \\
\mathbf{A_n}_{j,j} =& \frac{\chi}{(\Delta x)^2}\left(c_{j+1}^{k+1} - 2c_j^{k+1} + c_{j-1}^{k+1}\right) - \lambda_2 c_j^{k+1}\left(1 - n_j^k\right), \\
\mathbf{A_n}_{j,j+1} =& \frac{\chi}{(\Delta x)^2}\left(c_{j+1}^{k+1} - c_j^{k+1}\right),
\end{aligned}$$

where we have on the boundaries, due to the boundary conditions (3.2.3) and (3.3.4):

$$\begin{aligned}
\mathbf{A_n}_{1,1} =& \frac{\chi}{2(\Delta x)^2}\left(c_2^{k+1} - 2c_1^{k+1} + c_0^{k+1}\right) - \lambda_2 c_1^{k+1}\left(1 - n_1^{k+1}\right), \\
=& \frac{\chi}{(\Delta x)^2}\left(c_2^{k+1} - c_1^{k+1}\right) - \lambda_2 c_1^{k+1}\left(1 - n_1^{k+1}\right), \\
\mathbf{A_n}_{1,2} =& \frac{\chi}{2(\Delta x)^2}\left(c_2^{k+1} - c_1^{k+1}\right) + \frac{\chi}{2(\Delta x)^2}\left(c_0^{k+1} - c_1^{k+1}\right), \\
=& \frac{\chi}{(\Delta x)^2}\left(c_2^{k+1} - c_1^{k+1}\right), \\
\mathbf{A_n}_{N,N-1} =& \frac{\chi}{2(\Delta x)^2}\left(c_{N-1}^{k+1} - c_N^{k+1}\right) + \frac{\chi}{2(\Delta x)^2}\left(c_{N+1}^{k+1} - c_N^{k+1}\right), \\
=& \frac{\chi}{(\Delta x)^2}\left(c_{N-1}^{k+1} - c_N^{k+1}\right), \\
\mathbf{A_n}_{N,N} =& \frac{\chi}{2(\Delta x)^2}\left(c_{N+1}^{k+1} - 2c_N^{k+1} + c_{N-1}^{k+1}\right) - \lambda_2 c_N^{k+1}\left(1 - n_N^{k+1}\right), \\
=& \frac{\chi}{(\Delta x)^2}\left(c_{N-1}^{k+1} - c_N^{k+1}\right) - \lambda_2 c_N^{k+1}\left(1 - n_N^{k+1}\right).
\end{aligned}$$

And as last $\mathbf{b_n}$ in equation (5.5.2) equals

$$\mathbf{b_n} = \begin{pmatrix} \alpha_0 \rho_1^k c_1^{k+1} \\ \vdots \\ \alpha_0 \rho_j^k c_j^{k+1} \\ \vdots \\ \alpha_0 \rho_N^k c_N^{k+1} \end{pmatrix}. \tag{5.5.3}$$

Since Equation (3.5.3) contains no diffusion term we expect that the approximation derived above will contain oscillations. Therefore we will also determine the numerical approximations for Equation (3.5.3) with upwind discretization instead of central discretization for the boundary conditions. The steps to follow for the discretization are analoguous to above so we will not treat them.

5.5.1 Numerical simulatons and parameter values

Since the density of the stem cells and the concentration TG-beta are the same as in our first model we only consider the results for the capillary tip density.

We used the values from Table 5.5.1.

Name	Value	Description
Ω_w	0.2	Distance to core of the 'wound' in the heart
m_0	2	Initial density of stem cells
β	0.5	Decay of stem cells
D_1	1	Diffusion coefficient
α	3	Growth of TG-beta
λ	1	Decay of TG-beta
n_{eq}	0.01	Initial capillary tips density
χ	0.04	Attraction of TG-beta
λ_2	10	Growth and decay of the capillary tip density

Table 5.5.1: *Step sizes and values of the coefficients in the alternative model.*

Using the values from Table 5.5.1 we obtain the results for the capillary tip density as in Figure 5.5.1. In this figure some numerical approximations at different times t are plotted. At $t = 2$, the latest time, the capillary tip density is not yet decreasing. So the density increases in time in Figure 5.5.1.

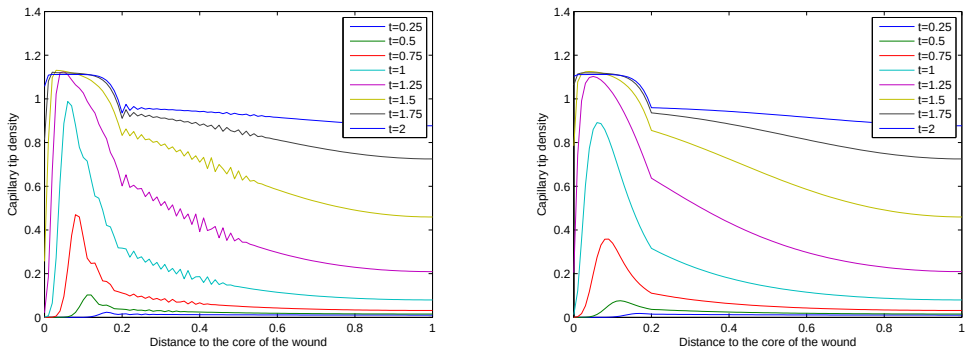

(a) Central discretization.

(b) Upwind discretization.

Figure 5.5.1: *Capillary tip density for the alternative model with two kinds of discretization for the convection terms for different times with* $\Delta x = 0.01$ $\Delta t = 0.01$ *and* $T = 2$.

We see that if we use a central discretization then spurious oscillations appear. This happens because Equation (3.5.3) is convection dominated. Therefore when we use an upwind discretization we retrieve a smooth approximation.

Since the alternative model is actually a simplification of our first model we will continue this research using our initial model.

Chapter 6

One dimensional finite element method

In Chapter 5 we used the finite difference method in order to find an approximation for our model as described in Chapter 3. The disadvantage of the finite difference method is that it is only applicable to rectangular shapes. Besides that, the finite difference method does not necessarily conserve quantities, it only replaces the derivatives with difference formulas.
Since the finite element method, as described in [4], can handle complicated geometries as well as conserving fluxes, this method can probably also give us a good approximation for our two dimensional problem. Therefore we now observe the results using the finite element method for our one dimensional problem.

In order to do so we partition our scaled domain $[0, 1]$ into N elements, $\{e_j\}_1^N$, and define $e_j = [x_{j-1}, x_j]$ such that each element has equal size $\Delta x = x_j - x_{j-1}$ $j = 1...N$. As our basisfunctions we use linear piecewise basisfunctions denoted by l and m as illustrated in Figure 6.0.1. The time points are again denoted by k and for the results of the stem cell density we use the exact solution from (4.1.1).

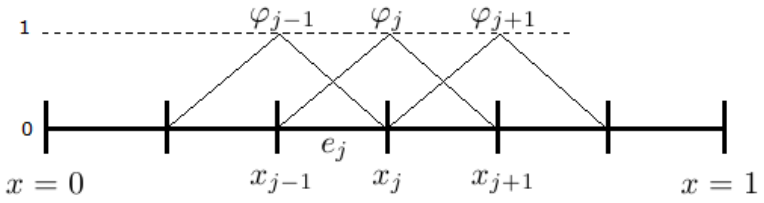

Figure 6.0.1: Piecewise linear basisfunctions

The first step in the finite element method is to determine the weak formulation. This is done by multiplying the equation by a test function $\varphi \in \Sigma$ where

$$\Sigma = \{\varphi \text{ sufficiently smooth} : \varphi(0) = 0\}, \tag{6.0.1}$$

and integrating this over the whole domain $[0, 1]$.

After finding the weak formulation we need to use Galerkin's method in order to find a approximation for our unknown, for example the concentration TG-beta. Therefore we need to approximate the solution by a linear combination of basisfunctions,

$$c \approx \sum_{l=1}^{N} c_l(t)\varphi_l(x), \tag{6.0.2}$$

ans replace the test function φ by each of the basic functions separately. The Galerkin method gives a formula for entries of the mass matrix, the stifness matrix and of the right handside vector for internal elements.

Note that for an element e_j only the basisfunctions that have their influence are the nonzero ones, namely φ_{j-1} and φ_j. Therefore the mass matrix, element matrix and the element vector on element e_j only depend on φ_{j-1} and φ_j.

The last step is to also find the element matrix and the element vector for boundary elements (the mass matrix is the same for internal and boundary elements). After finding these quantities for all elements, we need to combine everything into a final mass matrix, stiffness matrix source vector.

6.1 Concentration TG-beta

In this section we follow al the described steps for the finite element method on Equation (3.2.1) in order to find a numerical approximation.

6.1.1 Weak formulation

Following the steps to retrieve the weak formulation for Equation (3.2.1), we get

$$\int_0^1 \frac{\partial c}{\partial t}\varphi - D_1\frac{\partial^2 c}{\partial x^2}\varphi + \lambda c\varphi \; dx = \int_0^1 \alpha m\varphi \; dx,$$

where we apply partial integration to obtain

$$\int_0^1 \frac{\partial c}{\partial t}\varphi + D_1\frac{\partial c}{\partial x}\frac{d\varphi}{dx} + \lambda c\varphi \; dx = \int_0^1 \alpha m\varphi \; dx - D_1\frac{\partial c}{\partial x}(x)\varphi(x)\Big|_0^1,$$

which is due to the boundary conditions (3.2.3) equal to

$$\int_0^1 \frac{\partial c}{\partial t}\varphi + D_1\frac{\partial c}{\partial x}\frac{d\varphi}{dx} + \lambda c\varphi \; dx = \int_0^1 \alpha m\varphi \; dx, \quad \forall\varphi \in \Sigma. \tag{6.1.1}$$

Equation (6.1.1) is the so called weak formulation.

6.1.2 Galerkin method

Applying the steps of the Galerkin method Equation (6.1.1) becomes

$$\sum_{l=1}^{N} \int_0^1 \frac{dc_l}{dt}\varphi_l\varphi_m + D_1 c_l \frac{d\varphi_l}{dx}\frac{d\varphi_m}{dx} + \lambda c_l \varphi_l \varphi_m \, dx = \int_0^1 \alpha m \varphi_m \, dx,$$

$$\implies \sum_{l=1}^{N} \underbrace{\int_0^1 \varphi_m\varphi_l \, dx}_{M_{ml}} \frac{dc_l}{dt} = \sum_{l=1}^{N} \underbrace{\int_0^1 -D_1 \frac{d\varphi_m}{dx}\frac{d\varphi_l}{dx} - \lambda\varphi_m\varphi_l \, dx}_{S_{ml}} c_l + \underbrace{\int_0^1 \alpha m \varphi_m \, dx}_{f_m}. \tag{6.1.2}$$

Equation (6.1.2) shows we can solve Equation (3.2.1) with the finite element method by (6.1.3) with the help of the mass matrix M_{ml}, stiffness matrix S_{ml} and the source vector f_m using Euler backwards for the time integration.

$$Mc^{k+1} = Mc^k + \Delta t \left(Sc^{k+1} + f^k \right) \tag{6.1.3}$$

6.1.3 Mass matrix, stiffness matrix and source vector

Equation (6.1.2) shows us how the mass matrix, element matrix and the element vector look are constructed. The internal elements and the boundary elements will be slightly different since the boundary elements need to contain the boundary conditions given in (3.2.3).
As we know the mass matrix, element matrix and element vector depend only on φ_{j-1} and φ_j.

The mass matrix for internal and boundary elements look like:

$$\begin{aligned} M_m^{e_j} =& \int_{e_j} \varphi_m\varphi_l \, dx, \\ M^{e_j} =& \frac{\Delta x}{2} \begin{pmatrix} 1 & 0 \\ 0 & 1 \end{pmatrix}, \end{aligned}$$

such that

$$M = \frac{\Delta x}{2} \begin{pmatrix} 1 & & & & \\ & 2 & & \emptyset & \\ & & \ddots & & \\ & \emptyset & & 2 & \\ & & & & 1 \end{pmatrix}. \tag{6.1.4}$$

The element matrix for an internal element is:

$$\begin{aligned}
S^{e_j}_{ml} &= \int_{e_j} -D_1 \frac{d\varphi_m}{dx}\frac{d\varphi_l}{dx} - \lambda\varphi_m\varphi_l \; dx, \\
S^{e_j} &= \begin{pmatrix} \int_{e_j} -D_1 \frac{d\varphi_{j-1}}{dx}\frac{d\varphi_{j-1}}{dx} - \lambda\varphi_{j-1}\varphi_{j-1} \; dx & \int_{e_j} -D_1 \frac{d\varphi_{j-1}}{dx}\frac{d\varphi_j}{dx} - \lambda\varphi_{j-1}\varphi_j \; dx \\ \int_{e_j} -D_1 \frac{d\varphi_j}{dx}\frac{d\varphi_{j-1}}{dx} - \lambda\varphi_j\varphi_{j-1} \; dx & \int_{e_j} -D_1 \frac{d\varphi_j}{dx}\frac{d\varphi_j}{dx} - \lambda\varphi_j\varphi_j \; dx \end{pmatrix} \\
&= \begin{pmatrix} -\frac{D_1}{\Delta x} - \lambda\frac{\Delta x}{2} & \frac{D_1}{\Delta x} \\ \frac{D_1}{\Delta x} & -\frac{D_1}{\Delta x} - \lambda\frac{\Delta x}{2} \end{pmatrix},
\end{aligned}$$

where we used Newton Côtes numerical integration.
Combining this with the boundary conditions (3.2.3) gives the stiffness matrix

$$S = -\frac{D_1}{\Delta x}\begin{pmatrix} 1 & -1 & & & \\ -1 & 2 & -1 & & \emptyset \\ & & \ddots & & \\ \emptyset & & -1 & 2 & -1 \\ & & & -1 & 1 \end{pmatrix} - \lambda\frac{\Delta x}{2}\begin{pmatrix} 1 & & & & \\ & 2 & & \emptyset & \\ & & \ddots & & \\ & \emptyset & & 2 & \\ & & & & 1 \end{pmatrix}. \tag{6.1.5}$$

The element vector for an internal element is:

$$\begin{aligned}
f^{e_j}_m &= \int_{e_j} \alpha m\varphi_m \; dx, \\
f^{e_j} &= \begin{pmatrix} \int_{e_j} \alpha m\varphi_{j-1} \; dx \\ \int_{e_j} \alpha m\varphi_j \; dx \end{pmatrix} \\
&= \alpha\frac{\Delta x}{2}\begin{pmatrix} m(x_{j-1}, t) \\ m(x_j, t) \end{pmatrix},
\end{aligned}$$

where we have used Newton Côtes numerical integration such that

$$f = \alpha\frac{\Delta x}{2}\begin{pmatrix} m(x_0, t) \\ 2 \cdot m(x_1, t) \\ \vdots \\ 2 \cdot m(x_{N-1,t}) \\ m(x_N, t) \end{pmatrix}. \tag{6.1.6}$$

6.2 Capillary tip density

6.2.1 Weak formulation

To determine the weak formulation for the relatively complicated equation, Equation (3.3.1), we get

$$\int_0^1 \frac{\partial n}{\partial t}\varphi + \chi_1\frac{\partial}{\partial x}\left(n\frac{\partial c}{\partial x}\right)\varphi - D_2\frac{\partial^2 n}{\partial x^2}\varphi \; dx = \int_0^1 \alpha_0\rho c\varphi + \alpha_1 H\left(c - \hat{c}\right)nc\varphi - \beta_2 n\rho\varphi \; dx,$$

where we apply partial integration on two terms to obtain

$$\int_0^1 \frac{\partial n}{\partial t}\varphi + \chi_1 \frac{\partial n}{\partial x}\frac{\partial \varphi}{\partial x} - \chi_1 n \frac{\partial c}{\partial x}\frac{d\varphi}{dx} - \chi_1 \frac{\partial n}{\partial x}\frac{\partial \varphi}{\partial x} + D_2 \frac{\partial n}{\partial x}\frac{d\varphi}{dx}\, dx + \chi_1 n \frac{\partial c}{\partial x}\varphi\Big|_0^1 - D_2 \frac{\partial n}{\partial x}\varphi\Big|_0^1$$
$$= \int_0^1 \alpha_0 \rho c \varphi + \alpha_1 H\left(c - \hat{c}\right) n c \varphi - \beta_2 n \rho \varphi \, dx.$$

Applying the boundary conditions (3.2.3) and (3.3.4) we get

$$\int_0^1 \frac{\partial n}{\partial t}\varphi - \left(\chi_1 n \frac{\partial c}{\partial x} - D_2 \frac{\partial n}{\partial x}\right)\frac{d\varphi}{dx}\, dx$$
$$= \int_0^1 \alpha_0 \rho c \varphi + \alpha_1 H\left(c - \hat{c}\right) n c \varphi - \beta_2 n \rho \varphi \, dx, \ \forall \varphi \in \Sigma. \tag{6.2.1}$$

Equation (6.2.1) is the weak formulation.

6.2.2 Galerkin method

Applying the steps of the Galerkin method to Equation (6.2.1) we obtain

$$\sum_{l=1}^{N} \int_0^1 \frac{\partial n_l}{\partial t}\varphi_l \varphi_m - \chi_1 n_l \varphi_l \frac{\partial c}{\partial x}\frac{d\varphi_m}{dx} + D_2 n_l \frac{d\varphi_l}{dx}\frac{d\varphi_m}{dx}\, dx$$
$$= \sum_{l=1}^{N} \int_0^1 \alpha_1 H\left(c - \hat{c}\right) n_l \varphi_l c \varphi_m - \beta_2 n_l \varphi_l \rho \varphi_m \, dx + \int_0^1 \alpha_0 \rho c \varphi_m \, dx,$$

$$\Longrightarrow \sum_{l=1}^{N} \frac{dn_l}{dx} \underbrace{\int_0^1 \varphi_m \varphi_l \, dx}_{M_{ml}}$$
$$= \sum_{l=1}^{N} n_l \underbrace{\int_0^1 \chi_1 \frac{\partial c}{\partial x}\frac{d\varphi_m}{dx}\varphi_l - D_2 \frac{d\varphi_m}{dx}\frac{d\varphi_l}{dx} + \alpha_1 H\left(c - \hat{c}\right) c \varphi_m \varphi_l - \beta_2 \rho \varphi_m \varphi_l \, dx}_{S_{ml}} n_l$$
$$+ \underbrace{\int_0^1 \alpha_0 \rho c \varphi_m \, dx}_{f_m}. \tag{6.2.2}$$

We rewrite (6.2.2) into a matrix-vector equation to determine the approximations. Here we use the implicit Euler backwards for the time integration and since ρ^{k+1} depends on the solution of n_j^{k+1} we need to approximate it explicitly. Therefore we actually use the IMEX method.So in the equation for the capillary tip density ρ_j^{k+1} will be approximated by ρ_j^k. This is just as we did in Chapter 5. We obtain the matrix-vector equation

$$Mn^{k+1} = Mn^k + \Delta t \left(S(\rho^k)n^{k+1} + f^{k+1}\right) \tag{6.2.3}$$

6.2.3 Mass matrix, stiffness matrix and source vector

Since M_{ml} from Equation (6.2.2) is equal M_{ml} from Equation (6.1.2) the mass matrix is equal to (6.1.4).

The element matrix for an internal element is:

$$
\begin{aligned}
S_{ml}^{e_j} =& \int_{e_j} \chi_1 \frac{\partial c}{\partial x} \frac{d\varphi_m}{dx} \varphi_l - D_2 \frac{d\varphi_m}{dx} \frac{d\varphi_l}{dx} + \alpha_1 H\left(c-\hat{c}\right) c \varphi_m \varphi_l - \beta_2 \rho \varphi_m \varphi_l \, dx, \\
S^{e_j} =& \begin{pmatrix}
\int_{e_j} \chi_1 \frac{\partial c}{\partial x} \frac{d\varphi_{j-1}}{dx} \varphi_{j-1} - D_2 \frac{d\varphi_{j-1}}{dx} \frac{d\varphi_{j-1}}{dx} + & \int_{e_j} \chi_1 \frac{\partial c}{\partial x} \frac{d\varphi_{j-1}}{dx} \varphi_j - D_2 \frac{d\varphi_{j-1}}{dx} \frac{d\varphi_j}{dx} + \\
\alpha_1 H\left(c-\hat{c}\right) c \varphi_{j-1} \varphi_{j-1} - \beta_2 \rho \varphi_{j-1} \varphi_{j-1} \, dx & \alpha_1 H\left(c-\hat{c}\right) c \varphi_{j-1} \varphi_j - \beta_2 \rho \varphi_{j-1} \varphi_j \, dx \\
\int_{e_j} \chi_1 \frac{\partial c}{\partial x} \frac{d\varphi_j}{dx} \varphi_{j-1} - D_2 \frac{d\varphi_j}{dx} \frac{d\varphi_{j-1}}{dx} + & \int_{e_j} \chi_1 \frac{\partial c}{\partial x} \frac{d\varphi_j}{dx} \varphi_j - D_2 \frac{d\varphi_j}{dx} \frac{d\varphi_j}{dx} + \\
\alpha_1 H\left(c-\hat{c}\right) c \varphi_j \varphi_{j-1} - \beta_2 \rho \varphi_j \varphi_{j-1} \, dx & \alpha_1 H\left(c-\hat{c}\right) c \varphi_j \varphi_j - \beta_2 \rho \varphi_j \varphi_j \, dx
\end{pmatrix} \\
=& \chi_1 \begin{pmatrix}
\frac{\partial c}{\partial x}(x_{j-1},t) \frac{-1}{\Delta x} \frac{\Delta x}{2} & \frac{\partial c}{\partial x}(x_j,t) \frac{-1}{\Delta x} \frac{\Delta x}{2} \\
\frac{\partial c}{\partial x}(x_{j-1},t) \frac{1}{\Delta x} \frac{\Delta x}{2} & \frac{\partial c}{\partial x}(x_j,t) \frac{1}{\Delta x} \frac{\Delta x}{2}
\end{pmatrix} - \frac{D_2}{\Delta x} \begin{pmatrix} 1 & -1 \\ -1 & 1 \end{pmatrix} \\
&+ \frac{\Delta x}{2} \begin{pmatrix} g(x_{j-1},t) & 0 \\ 0 & g(x_j) \end{pmatrix}.
\end{aligned}
$$

where we have used Newton Côtes numerical integration, the definition

$$
g(x_j,t) = \alpha_1 H\left(c(x_j,t)-\hat{c}\right) c(x_j,t) - \beta_2 \rho(x_j,t), \tag{6.2.4}
$$

and the approximation

$$
\frac{\partial c}{\partial x} = \frac{c_{j+1}-c_{j-1}}{2\Delta x}. \tag{6.2.5}
$$

Applying boundary conditions (3.2.3) and (3.3.4) and the definition (6.2.4) we get the stiffness matrix

$$
S = \frac{\chi_1}{2} \begin{pmatrix}
0 & \frac{\partial c}{\partial x}(x_1,t) & & & \\
-\frac{\partial c}{\partial x}(x_0,t) & \ddots & \ddots & & \emptyset \\
& \ddots & \ddots & \ddots & \\
\emptyset & & \ddots & \ddots & \frac{\partial c}{\partial x}(x_N,t) \\
& & & -\frac{\partial c}{\partial x}(x_{N-1},t) & 0
\end{pmatrix}
$$

$$
\begin{aligned}
&- \frac{D_2}{\Delta x}
\begin{pmatrix}
1 & -1 & & & \\
-1 & 2 & -1 & & \emptyset \\
 & & \ddots & & \\
\emptyset & & -1 & 2 & -1 \\
 & & & -1 & 1
\end{pmatrix} \\
&+ \frac{\Delta x}{2}
\begin{pmatrix}
g(x_0,t) & & & & \\
 & 2\cdot g(x_1,t) & & \emptyset & \\
 & & \ddots & & \\
 & \emptyset & & 2\cdot g(x_{N-1},t) & \\
 & & & & g(x_N,t)
\end{pmatrix}.
\end{aligned} \tag{6.2.6}
$$

The element vector for an internal element is:

$$
\begin{aligned}
f_m^{e_j} &= \int_{e_j} \alpha_0 \rho c \varphi_m \, dx, \\
f^{e_j} &= \frac{\Delta x}{2}
\begin{pmatrix}
\alpha_0 \rho(x_{j-1}) c(x_{j-1}) \\
\alpha_0 \rho(x_j) c(x_j)
\end{pmatrix},
\end{aligned}
$$

where we used Newton Côtes numerical integration such that by adding boundary condition (3.4.3) the source vector becomes

$$
f = \frac{\alpha_0 \Delta x}{2}
\begin{pmatrix}
\rho(x_0,t)c(x_0,t) \\
2\cdot \rho(x_1,t)c(x_1,t) \\
\vdots \\
2\cdot \rho(x_{N-1},t)c(x_{N-1},t) \\
\rho_{eq} c(x_N,t)
\end{pmatrix}. \tag{6.2.7}
$$

6.3 Vessel density

6.3.1 Weak formulation

By multiplying by a test function $\varphi \in \Sigma$ and by integrating over the domain of computation we get

$$
\int_0^1 \frac{\partial \rho}{\partial t}\varphi - \epsilon \frac{\partial^2 \rho}{\partial x^2}\varphi + \gamma\rho\varphi - \gamma\rho_{eq}\varphi \, dx = \int_0^1 \mu_1 \frac{\partial n}{\partial x}\varphi - \chi_2 n \frac{\partial c}{\partial x}\varphi \, dx,
$$

where we apply partial integration to obtain

$$
\int_0^1 \frac{\partial \rho}{\partial t}\varphi + \epsilon \frac{\partial \rho}{\partial x}\frac{d\varphi}{dx} + \gamma\rho\varphi \, dx - \epsilon \frac{\partial \rho}{\partial x}\varphi \Big|_0^1 = \int_0^1 \mu_1 \frac{\partial n}{\partial x}\varphi - \chi_2 n \frac{\partial c}{\partial x}\varphi + \gamma\rho_{eq}\varphi \, dx
$$

which becomes, due to the boundary conditions (3.4.3) and the fact that $\varphi(1) = 0$ since $\rho(1,t)$ is known

$$
\int_0^1 \frac{\partial \rho}{\partial t}\varphi + \epsilon \frac{\partial \rho}{\partial x}\frac{d\varphi}{dx} + \gamma\rho\varphi \, dx = \int_0^1 \mu_1 \frac{\partial n}{\partial x}\varphi - \chi_2 n \frac{\partial c}{\partial x}\varphi + \gamma\rho_{eq}\varphi \, dx, \ \forall \varphi \in \Sigma. \tag{6.3.1}
$$

Equation (6.3.1) is the weak formulation.

6.3.2 Galerkin method

Applying the Galerkin method to Equation (6.3.1) we get

$$\sum_{l=1}^{N} \int_0^1 \frac{d\rho_l}{dt}\varphi_l\varphi_m + \epsilon\rho_l \frac{d\varphi_l}{dx}\frac{d\varphi_m}{dx} + \gamma\rho_l\varphi_l\varphi_m \; dx = \int_0^1 \mu_1 \frac{\partial n}{\partial x}\varphi_m - \chi_2 n \frac{\partial c}{\partial x}\varphi_m + \gamma\rho_{eq}\varphi_m \; dx,$$

$$\begin{aligned} \implies \sum_{l=1}^{N} \underbrace{\int_0^1 \varphi_m\varphi_l \; dx}_{M_{ml}} \frac{d\rho_l}{dt} = &\sum_{l=1}^{N} \underbrace{\int_0^1 -\epsilon\frac{d\varphi_m}{dx}\frac{d\varphi_l}{dx} - \lambda\varphi_m\varphi_l \; dx}_{S_{ml}} \rho_l \\ &+ \underbrace{\int_0^1 \mu_1\frac{\partial n}{\partial x}\varphi_m - \chi_2 n\frac{\partial c}{\partial x}\varphi_m + \gamma\rho_{eq}\varphi_m \; dx}_{f_m}. \end{aligned} \tag{6.3.2}$$

From Equation (6.3.2) we can solve Equation (3.4.1) with the mass matrix M_{ml}, element matrix S_{ml} and the element vector f_m using the Euler backwards method for the time integration:

$$M\rho^{k+1} = M\rho^k + \Delta t\left(S\rho^{k+1} + f^{k+1}\right) \tag{6.3.3}$$

6.3.3 Mass matrix, stiffness matrix and source vector

To solve Equation (6.3.3), we need to know exactly the mass matrix, stiffness matrix and source vector. Therefore, we first construct the element matrix and vector and then substitute these quantities into the stiffness matrix and source, upon vector taking into account the boundary conditions.

Since the mass matrix is identical to the mass matrix from the concentration TG-beta it is equal to (6.1.4).

The element matrix for an internal element is:

$$\begin{aligned} S^{e_j}_{ml} &= \int_{e_j} -\epsilon\frac{d\varphi_m}{dx}\frac{d\varphi_l}{dx} - \gamma\varphi_m\varphi_l \; dx, \\ S^{e_j} &= \begin{pmatrix} \int_{e_j} -\epsilon\frac{d\varphi_{j-1}}{dx}\frac{d\varphi_{j-1}}{dx} - \gamma\varphi_{j-1}\varphi_{j-1} \; dx & \int_{e_j} -\epsilon\frac{d\varphi_{j-1}}{dx}\frac{d\varphi_j}{dx} - \gamma\varphi_{j-1}\varphi_j \; dx \\ \int_{e_j} -\epsilon\frac{d\varphi_j}{dx}\frac{d\varphi_{j-1}}{dx} - \gamma\varphi_j\varphi_{j-1} \; dx & \int_{e_j} -\epsilon\frac{d\varphi_j}{dx}\frac{d\varphi_j}{dx} - \gamma\varphi_j\varphi_j \; dx \end{pmatrix} \\ &= \begin{pmatrix} -\frac{\epsilon}{\Delta x} - \gamma\frac{\Delta x}{2} & \frac{\epsilon}{\Delta x} \\ \frac{\epsilon}{\Delta x} & -\frac{\epsilon}{\Delta x} - \gamma\frac{\Delta x}{2} \end{pmatrix}, \end{aligned}$$

where we used Newton Côtes numerical integration. Since the value for $\rho(x_N, t)$ is given in the boundary condition, the approximation for that element is eliminated from the matrix. By doing so and by applying the boundary conditions (3.4.3), the $(N-1) \times (N-1)$ stiffness matrix is obtained:

$$S = -\frac{\epsilon}{\Delta x}\begin{pmatrix} 1 & -1 & & & \\ -1 & 2 & -1 & & \emptyset \\ & & \ddots & & \\ \emptyset & & -1 & 2 & -1 \\ & & & -1 & 2 \end{pmatrix} - \frac{\gamma\Delta x}{2}\begin{pmatrix} 1 & & & \\ & 2 & & \emptyset \\ & & \ddots & \\ & \emptyset & & 2 \end{pmatrix}. \tag{6.3.4}$$

Because the size of the stiffness matrix is now $(N-1)\times(N-1)$, the value in the source vector for element e_{N-1} contains an extra term. The element vector for an internal element becomes:

$$\begin{aligned} f_m^{e_j} &= \int_{e_j} \mu_1 \frac{\partial n}{\partial x}\varphi_m - \chi_2 n \frac{\partial c}{\partial x}\varphi_m + \gamma\rho_{eq}\varphi_m \, dx, \\ f^{e_j} &= \begin{pmatrix} \int_{e_j} \mu_1 \frac{\partial n}{\partial x}\varphi_{j-1} - \chi_2 n \frac{\partial c}{\partial x}\varphi_{j-1} + \gamma\rho_{eq}\varphi_{j-1} \, dx \\ \int_{e_j} \mu_1 \frac{\partial n}{\partial x}\varphi_j - \chi_2 n \frac{\partial c}{\partial x}\varphi_j + \gamma\rho_{eq}\varphi_j \, dx \end{pmatrix} \\ &= \frac{\Delta x}{2}\begin{pmatrix} \mu_1 \frac{\partial n}{\partial x}(x_{j-1}) - \chi_2 n(x_{j-1})\frac{\partial c}{\partial x}(x_{j-1}) + \gamma\rho_{eq} \\ \mu_1 \frac{\partial n}{\partial x}(x_j) - \chi_2 n(x_j)\frac{\partial c}{\partial x}(x_j) + \gamma\rho_{eq} \end{pmatrix}, \end{aligned}$$

where we have used Newton Côtes numerical integration such that the total source vector equals

$$f = \frac{\Delta x}{2}\begin{pmatrix} \mu_1 \frac{\partial n}{\partial x}(x_1) - \chi_2 n(x_1)\frac{\partial c}{\partial x}(x_1) + \gamma\rho_{eq} \\ 2\cdot\left(\mu_1 \frac{\partial n}{\partial x}(x_2) - \chi_2 n(x_2)\frac{\partial c}{\partial x}(x_2) + \gamma\rho_{eq}\right) \\ \vdots \\ \vdots \\ 2\cdot\left(\mu_1 \frac{\partial n}{\partial x}(x_{N-1}) - \chi_2 n(x_{N-1})\frac{\partial c}{\partial x}(x_{N-1}) + \gamma\rho_{eq}\right) \end{pmatrix} + \begin{pmatrix} 0 \\ \vdots \\ \vdots \\ 0 \\ \frac{\epsilon}{\Delta x}\rho_{eq} \end{pmatrix}. \tag{6.3.5}$$

6.4 Numerical simulations

Since we approximate the same model as before we use the values for the coefficients as given in Table 5.4.1.

In Figure 6.1(a) we see the results for the concentration TG-beta. When we compare the results from the finite element method with the results from the finite difference method,we observe that the finite element method always gives a result slightly different from the finite difference method. In Figures 6.1(b) and 6.1(c) we see that this is also the case for the capillary tip density and the vessel density upon comparing them to Figures 5.4.3 and 5.4.4.

The steady-states for our equations are of course the same for the finite difference method and the finite element method. Convergence to the steady-state for the finite element

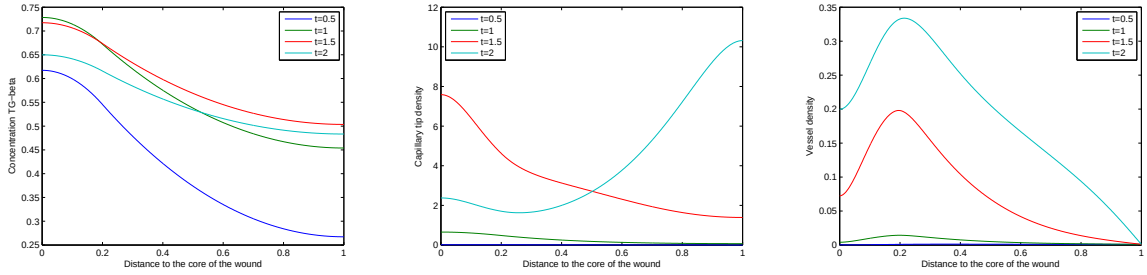

(a) Concentration TG-beta (b) Capillary tip density (c) Vessel density

Figure 6.4.1: *Simulations with* $\Delta x = 0.001,\ \Delta t = 0.01$ *and* $T = 2$.

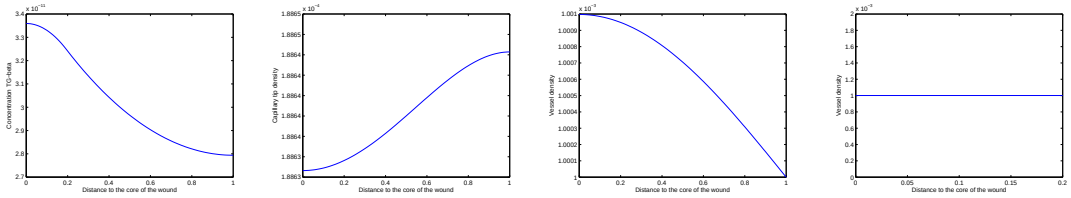

(a) Concentration TG-beta (b) Capillary tip density (c) Vessel density (d) Vessel density in the wound

Figure 6.4.2: *Values after* $T = 50$ *with* $\Delta x = 0.01$ *and* $\Delta t = 0.1$.

method is shown in Figure 6.4.2 where we again see that after the injection of stem cells an equilibrium of the capillary tip density is formed in the wound of the heart.

To show that the difference between te results of the finite difference method and the finite element method are indeed very small we determined the maximum relative difference between the two methods for all three equations. This has been done in Table 6.4.1, where the minimal relative error is given by

$$\max\left\{\frac{\|x^t_{\text{fdm}} - x^t_{\text{fem}}\|_1}{\max\{\|x^t_{\text{fdm}}\|_1, \|x^t_{\text{fem}}\|_1\}}\right\},$$

for $x = c,\ x = n,\ x = \rho$ and different times t.
As we can see in Table 6.4.1 the differences are indeed relatively small. Only the difference for the vessel density is relatively large, however this can be explained.

In the finite difference method we used a central discretization for the spatial part also at the boundaries. Therefore we have introduced two ghost points, one to the left of $x = 0$ and one to the right of $x = 1$. The boundary condition $\rho(1, t) = \rho_{eq}$ is therefore applied to the ghost point at the right from $x = 1$, on the point x_{N+1}. Because of the ghost point the approximated value $\rho(x_N, t)$ is not ρ_{eq}.
For the finite element method we did not introduce any ghost cells. We have left the

	$\Delta x = 0.01$			$\Delta x = 0.001$			$\Delta x = 0.0005$		
	c	n	ρ	c	n	ρ	c	n	ρ
$t = 0.5$	0.0100	0.0282	0.0151	0.0100	0.0286	0.0156	0.0100	0.0286	0.0156
$t = 1.0$	0.0100	0.0567	0.0537	0.0100	0.0574	0.0548	0.0100	0.0575	0.0548
$t = 1.5$	0.0100	0.0559	0.2738	0.0100	0.0567	0.0566	0.0100	0.0567	0.0566
$t = 2.0$	0.0100	0.0389	0.7976	0.0100	0.0366	0.2712	0.0100	0.0365	0.2166

Table 6.4.1: *Maximum relative difference between the finite difference method (with Δx between the points) and the finite element method (with element size Δx).*

last cell, cell e_N, out of our numerical computation because we have inserted the known value ρ_{eq} there.
Over time, the vessel density in x_N gets bigger (and later it reduces again) for the finite difference method and the vessel density stays equal to ρ_{eq} in the finite element method. Therefore the difference in x_N gets larger for these two methods. So this difference does not follow from the methods but from the way we have implemented them. Notice that when we increase the number of elements, and therefore decrease the size of the elements, the relative difference between the two methods gets smaller.

Chapter 7

One dimensional finite element method with SUPG

7.1 Dominated by convection

When using a method like the finite element method it is necessary to investigate whether the equation is diffusion dominated, convection dominated or a little of both. If the method is dominated by convection for some values of the speed and the diffusion coefficient, then there is a possibility that a numerical method will fail. Upwinding will be needed. We can use the Péclet number to determine which part of the equation dominates it.

Consider the scalar advection diffusion equation

$$\frac{\partial u}{\partial t} + v\nabla u - D\Delta u = 0, \tag{7.1.1}$$

where v is the speed and D is the diffusion coefficient. The Péclet equation for Equation (7.1.1) is given by

$$Pe = \frac{v\Delta x}{D}, \tag{7.1.2}$$

where Δx is the step size of the space-discretization.

With the value of Pe we know wether it is dominated by diffusion, convection or both [8].

$Pe = 0$,	pure diffusion,
$Pe \leq 1$,	diffusion-dominated,
$1 < Pe \leq 10$,	both are important,
$Pe > 10$,	convection-dominated,
$Pe = \infty$,	pure convection.

7.2 Streamline Upwind Petrov-Galerkin

Using the finite element method to an equation dominated by convection, some numerical diffusion will occur and it is possible that our numerical method will fail. In order to neutralize the numerical diffusion we can use the streamline upwind Petrov-Galerkin method, abbreviated by SUPG. SUPG is similar to the finite element method. Only now we multiply by the test function $\eta(x)$, which is the sum of the classical test function $\varphi(x)$ from the finite element method which is in the same function space as the solution, and an extra test function $p(x)$ which is not in the same function space as the solution ($\eta(x) = \varphi(x) + p(x)$). For example, if we have the equation

$$u_t + u_x = 0,$$

then the weak formulation becomes

$$\int_\Omega (u_t + u_x)\varphi(x)dx + \int_\Omega (u_t + u_x)p(x)\ dx = 0,$$

where the first part is from the weak formulation when using the common finite element method and the second part is the extra term when using this upwinding method.

We choose $p(x) = \frac{\Delta x}{2}\xi\frac{d\varphi_m}{dx}$, where ξ equals the sign of the speed.

7.3 Examples with SUPG

To show the numerical diffusion that can occur with the finite element method we treat a few examples where we apply streamline upwind Petrov-Galerkin to.

Advection equation: Standard Galerkin Method (SGM)

First we apply the finite element method to the advection equation. This equation equals

$$u_t + u_x = 0,$$

with boundary condition $u(0,t) = a$, where $a \in \mathbb{R}$, and initial condition $u(x,0) = g(x)$. Applying the finite element method we multiply the equation by a testfunction $\eta(x)$, subject to $\varphi(0) = 0$ since we have a Dirichlet boundary condition, and we integrate it over our domain $[0,1]$ to obtain

$$\int_0^1 u_t\varphi\ dx = -\int_0^1 u_x\varphi\ dx. \tag{7.3.1}$$

We approximate our solution by $u \approx \sum_{j=1}^N u_j\varphi_j + a\varphi_0$, where N is our number of elements and φ_l a basisfunction. Equation (7.3.1) becomes

$$\sum_{l=1}^N \frac{du_l}{dx}\int_0^1 \varphi_l\varphi_m\ dx = \sum_{l=1}^N u_l\int_0^1 -\frac{d\varphi_l}{dx}\varphi_m\ dx. \tag{7.3.2}$$

We use piecewise linear elements and all elements have the same size dx. The element mass matrix becomes

$$M^{e_j} = \frac{\Delta x}{2}\begin{pmatrix} 1 & 0 \\ 0 & 1 \end{pmatrix}, \tag{7.3.3}$$

and the element stiffness matrix becomes

$$S^{e_j} = \frac{1}{2}\begin{pmatrix} 1 & -1 \\ 1 & -1 \end{pmatrix}. \tag{7.3.4}$$

The element vector is the zero vector except for our left boundary, there the source vector equals

$$f^{e_l} = \begin{pmatrix} a/2 \\ 0 \\ \vdots \\ 0 \end{pmatrix}. \tag{7.3.5}$$

Advection equation with SUPG

As explained in Chapter 7.2 we apply the SUPG method by adding some terms to our mass matrix, stiffness matrix and source vector. These terms are determined by applying the advection equation by a different testfunction. We focus on the terms

$$\int_0^1 u_t p \; dx + \int_0^1 u_x p \; dx, \tag{7.3.6}$$

Again we approximate our solution by $u \approx \sum_{j=1}^{N} u_j \varphi_j + a\varphi_0$. Now we use

$$p(x) = \frac{\Delta x}{2}\xi \frac{d\varphi_m}{dx},$$

where ξ equals the sign of the speed. The terms from 7.3.6) become

$$\sum_{l=1}^{N} \frac{du_l}{dt}\frac{\Delta x}{2}\xi \int_0^1 \varphi_l \frac{d\varphi_m}{dx} \; dx + \sum_{l=1}^{N} u_l \frac{\Delta x}{2}\xi \int_0^1 \frac{d\varphi_l}{dx}\frac{d\varphi_m}{dx} \; dx. \tag{7.3.7}$$

From these relations we can determine the extra terms from SUPG. For the element mass matrix, the extra term, $M_p^{e_j}$, equals

$$M_p^{e_j} = \frac{\Delta x}{4}\xi \begin{pmatrix} -1 & -1 \\ 1 & 1 \end{pmatrix}, \tag{7.3.8}$$

and the extra term for our element stiffness matrix, $S_p^{e_j}$ is

$$S_p^{e_j} = \frac{1}{2}\xi \begin{pmatrix} -1 & 1 \\ 1 & -1 \end{pmatrix}. \tag{7.3.9}$$

Finally, we have the extra term for our source vector, f_p, which is

$$f^{e_l} = \begin{pmatrix} \xi\frac{a}{2} \\ 0 \\ \vdots \\ 0 \end{pmatrix}. \tag{7.3.10}$$

Perturbed advection equation with SGM

Next we apply the finite element method to a perturbed advection equation. This equation reads as

$$u_t + u_x = \epsilon u_{xx},$$

with boundary conditions $u(0,t) = a$ and $\frac{\partial u}{\partial x}(1,t) = b$, where $a, b \in \mathbb{R}$, and initial condition $u(x,0) = g(x)$. We multiply the equation by a testfunction $\varphi(x)$, subject to $\varphi(0) = 0$ since we have a Dirichlet boundary condition, and we integrate over a domain $[0,1]$ to obtain

$$\int_0^1 u_t\varphi \; dx = -\int_0^1 u_x\varphi + \epsilon\int_0^1 u_{xx}\varphi \; dx, \tag{7.3.11}$$

Applying partial integration to (7.3.11), gives

$$\int_0^1 u_t\varphi \; dx = -\int_0^1 u_x\varphi - \epsilon\int_0^1 u_x\varphi_x \; dx + \epsilon b\varphi(1), \tag{7.3.12}$$

We approximate the solution by $u \approx \sum_{j=1}^{N} u_j\varphi_j + a\varphi_0$, where N is the number of nodes and φ_l a basisfunction. Equation (7.3.12) becomes

$$\sum_{l=1}^{N} \frac{du_l}{dt}\int_0^1 \varphi_l\varphi_m \; dx = \sum_{l=1}^{N} u_l \int_0^1 -\frac{d\varphi_l}{dx}\varphi_m - \epsilon\frac{d\varphi_l}{dx}\frac{d\varphi_m}{dx} \; dx + \epsilon b\varphi_m(1). \tag{7.3.13}$$

Again we use piecewise linear elements and all elements still have the same size dx. The element mass matrix stays the same as for the advection equation, but the element stiffness matrix becomes

$$S^{e_j} = \frac{1}{2}\begin{pmatrix} 1 & -1 \\ 1 & -1 \end{pmatrix} + \frac{\epsilon}{\Delta x}\begin{pmatrix} -1 & 1 \\ 1 & -1 \end{pmatrix}. \tag{7.3.14}$$

The element vector is the zero vector except for our boundary elements. Therefore the source vector equals

$$f^{e_l} = \begin{pmatrix} \frac{a}{2} + \frac{\epsilon}{\Delta x}a \\ 0 \\ \vdots \\ 0 \\ \epsilon b \end{pmatrix}. \tag{7.3.15}$$

Perturbed advection equation with SUPG

In comparison to the advection equation, we only have the term $\epsilon \int_0^1 u_{xx}(\varphi + p)\ dx$ in addition. The SUPG part of this additional term will be zero since we use piecewise linear basisfunctions. Therefore, the additional term the our element mass matrix, element stiffness matrix and the source vector are the same as we derived for the advection equation.

Spatial differential equation

As an example we also tread the equation

$$-\epsilon u_{xx} + u_x = 0, \tag{7.3.16}$$

with boundary conditions $u(0) = 0$ and $u(1) = 1$. Since we have two Dirichlet boundary conditions the test function is subject to $\varphi(0) = \varphi(1) = 0$. We obtain

$$\int_0^1 -\epsilon u_{xx}\varphi + u_x\varphi\ dx = 0,$$

and applying partial integration this becomes

$$\int_0^1 \epsilon u_x\varphi_x + u_x\varphi\ dx = 0,$$

due to the properties of the test function. Using the approximation we obtain

$$\int_{l=1}^N u_l \int_0^1 \epsilon \frac{d\varphi_l}{dx}\frac{d\varphi_m}{dx} + \frac{d\varphi_l}{dx}\varphi_m\ dx = 0.$$

Therefore the Stiffness matrix becomes

$$S^{e_j} = \frac{\epsilon}{\Delta x}\begin{pmatrix} 1 & -1 \\ -1 & 1 \end{pmatrix} + \frac{1}{2}\begin{pmatrix} -1 & 1 \\ -1 & 1 \end{pmatrix}.$$

The solution for $u(x,t)$ can be found by solving

$$Su = f,$$

where f is the source vector which only contains some nonzero values in order to meet the boundary conditions.

Spatial differential equation with SUPG

The only extra term using SUPG comes from the term $\int_0^1 u_x p(x)\ dx$ since the other term is zero because of the linear basisfunctions that are used. We get

$$\sum_{l=1}^N u_l \int_0^1 \frac{\Delta x}{2}\xi \frac{d\varphi_l}{dx}\frac{d\varphi_m}{dx}\ dx,$$

such that

$$S_{p_{ml}}^{e_j} = \frac{\Delta x}{2} \frac{d\varphi_l}{dx} \frac{d\varphi_m}{dx} \Delta x.$$

Therefore the element matrix is given by

$$S_p^{e_j} = \frac{1}{2} \begin{pmatrix} 1 & -1 \\ -1 & 1 \end{pmatrix}.$$

7.4 Results

For the comparison between the finite element method without and with SUPG, we introduce two different initial conditions that we use:

$$u(x,0) = \begin{cases} 5 & x \leq 0.5, \\ 0 & \text{else}, \end{cases} \tag{7.4.1}$$

$$u(x,0) = 5 + \sin(2\pi x). \tag{7.4.2}$$

In the following figures we used the step size $\Delta x = 0.01$ and time step $\Delta t = 0.005$. Besides the approximation for $u(x,t)$ also the exact solutions are shown.

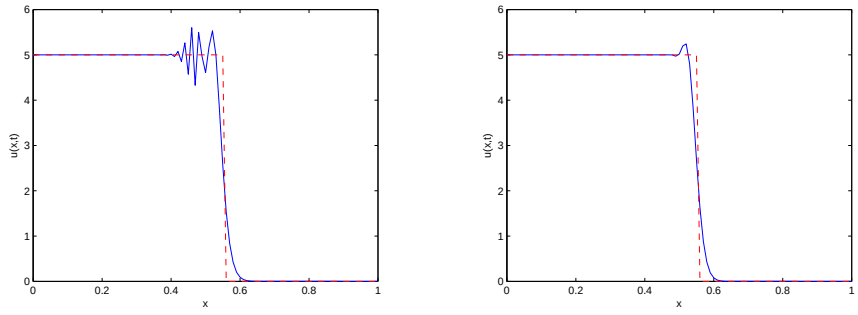

(a) Without SUPG (b) With SUPG

Figure 7.4.1: *Solution of (7.3.1) with initial condition (7.4.1) after 10 time steps.*

In Figure 7.4.1 we see the solution to the advection equation with a discontinuous initial condition. Without the use of SUPG, the approximation clearly shows wiggles and smearing around the point of discontinuity. Using SUPG there is only one wiggle left so this is a good improvement.

A disadvantage of the SUPG method is that it is applied to the whole domain. In Figure 7.4.2 it appears that there is no difference in the approximation whether or not SUPG is used. In fact, using SUPG gives for some point a better approximation, whereas for other points a worse approximation is obtained. An improvement can be to apply SUPG

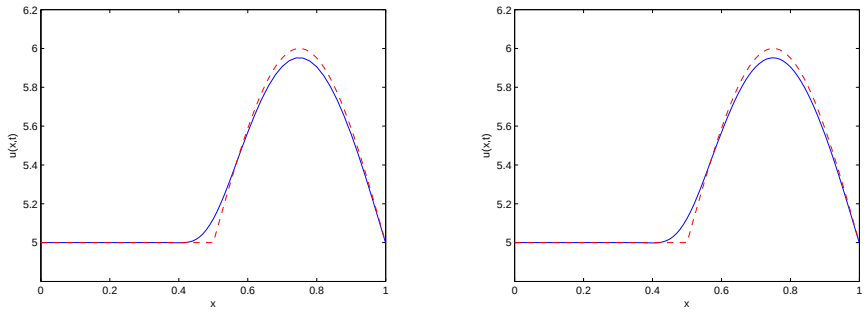

(a) Without SUPG (b) With SUPG

Figure 7.4.2: *Solution of (7.3.1) with initial condition (7.4.2) after 100 time steps.*

only on those elements where needed. In order to do so, wiggles and smearing should be detected.

For the perturbed advection equation we have done the same tests. In Figure 7.4.3, it appears that there is no difference between the approximations with and without SUPG. But in reality there is, with the use of SUPG there is less smearing in the approximation.

In Figure 7.4.4, it again appears that there is no difference between the approximations with and without SUPG. This is correct, SUPG hardly effects the solution here.

And in Figure 7.4.5 we have the solution to (7.3.16) with and without SUPG. Here the approximation without SUPG was already very good, so SUPG is actually not needed. In fact, using SUPG makes the approximation worse.

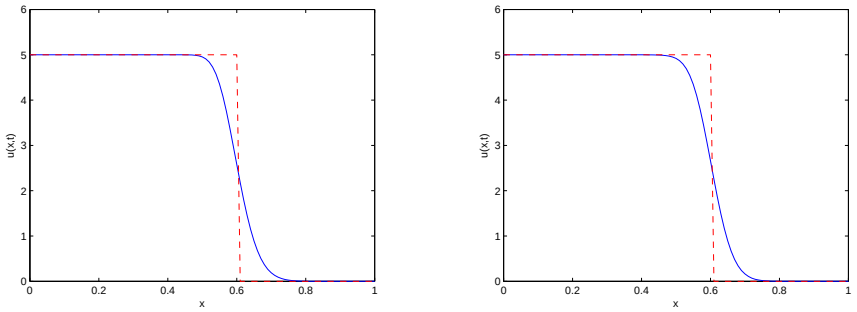

(a) Without SUPG (b) With SUPG

Figure 7.4.3: *Solution of (7.3.11) with initial condition (7.4.1) after 20 time steps with* $\epsilon = 0.01$.

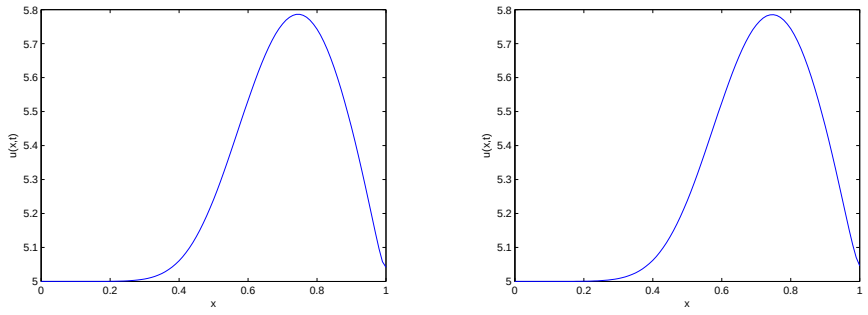

(a) Without SUPG (b) With SUPG

Figure 7.4.4: *Solution of (7.3.11) with initial condition (7.4.2) after 100 time steps with* $\epsilon = 0.01$.

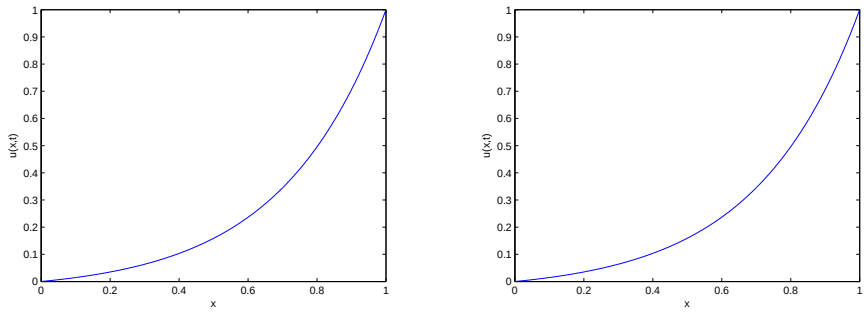

(a) Without SUPG (b) With SUPG

Figure 7.4.5: *Solution of (7.3.16).*

Concluding, one should know that SUPG does not always improve the quality of the solution.

7.5 SUPG to our model

For our model we need to apply SUPG to the equation for the capillary tip density. Inserting the test function $\eta(x) = \varphi(x) + p(x)$, the extra term equals

$$\int_0^1 \frac{\partial n}{\partial t} p + \chi_1 \frac{\partial}{\partial x}\left(n \frac{\partial c}{\partial x}\right) p - D_2 \frac{\partial^2 n}{\partial x^2} p \; dx = \int_0^1 \alpha_0 \rho c p + \alpha_1 H\left(c - \hat{c}\right) n c p - \beta_2 n \rho p \; dx.$$

Here we apply the partial integration

$$\int_0^1 -D_2 \frac{\partial^2 n}{\partial x^2} p \; dx = -D_2 \frac{\partial n}{\partial x} p \Big|_0^1 + D_2 \int_0^1 \frac{\partial n}{\partial x} \frac{dp}{dx} \; dx = 0,$$

which is zero due to the boundary conditions (3.3.4) and the fact that $\frac{dp}{dx} = \frac{\Delta x}{2}\xi\frac{d}{dx}\frac{d\varphi_m}{dx} = 0$, to obtain

$$\int_0^1 \frac{\partial n}{\partial t}p + \chi_1\frac{\partial}{\partial x}\left(n\frac{\partial c}{\partial x}\right)p\ dx = \int_0^1 \alpha_0\rho cp + \alpha_1 H\left(c-\hat{c}\right)ncp - \beta_2 n\rho p\ dx.$$

Applying the steps of the Galerkin method, substituting $p(x) = \frac{\Delta x}{2}\xi\frac{d\varphi_m}{dx}$ and using the product rule we get

$$\begin{aligned}
&\sum_{l=1}^{N}\frac{dn_l}{dt}\frac{\Delta x}{2}\xi\int_0^1 \varphi_l\frac{d\varphi_m}{dx}\ dx \\
&= \sum_{l=1}^{N} n_l\frac{\Delta x}{2}\xi\int_0^1\left(-\chi_1\frac{d\varphi_l}{dx}\frac{\partial c}{\partial x} - \chi_1\varphi_l\frac{\partial^2 c}{\partial x^2} + \alpha_1 H\left(c-\hat{c}\right)c\varphi_l - \beta_2\varphi_l\rho\right)\frac{d\varphi_m}{dx}\ dx \\
&+ \frac{\Delta x}{2}\xi\int_0^1 \alpha_0\rho c\frac{d\varphi_m}{dx}\ dx.
\end{aligned}$$

From this we can determine a mass matrix M_p, a stiffness matrix S_p and a source vector f_p. The matrices and vector obtained for the part with the classical test function are obtained in Chapter 6.2.3 and are respectively M_φ, S_φ and f_φ. The 'total' mass matrix, stiffness matrix and source vector are now equal to

$$\begin{aligned}
M &= M_\varphi + M_p, \\
S &= S_\varphi + S_p, \\
f &= f_\varphi + f_p.
\end{aligned}$$

The values for the capillary tip density can now be determined by

$$Mn^{k+1} = Mn^k + \Delta t(Sn^{k+1} + f^{k+1}).$$

Next we determine M_p, S_p and f_p. First the mass matrix:

$$M_{p_{ml}}^{e_j} = \frac{\Delta x}{2}\xi\int_{e_j}\varphi_l\frac{d\varphi_m}{dx}\ dx,$$

where

$$\frac{d\varphi_m}{dx} = \begin{cases} \frac{-1}{\Delta x} & m = j-1, \\ \\ \frac{1}{\Delta x} & m = j. \end{cases}$$

Substituting $\int_0^1 \varphi_l\ dx = \frac{\Delta x}{2}$ for $l = j-1, j$ we obtain

$$M_p^{e_j} = \frac{\Delta x}{4}\xi\begin{pmatrix} -1 & -1 \\ 1 & 1 \end{pmatrix}. \tag{7.5.1}$$

Next the stiffness matrix: Here we define the function $g(x,t)$ as we did in Chapter 6.2.3.

$$\begin{aligned}
S_{p_{ml}}^{e_j} =& \frac{\Delta x}{2}\xi \int_{e_j} \left(-\chi_1 \frac{d\varphi_l}{dx}\frac{\partial c}{\partial x} - \chi_1 \varphi_l \frac{\partial^2 c}{\partial x^2} + \underbrace{\alpha_1 H\left(c-\hat{c}\right) c\varphi_l - \beta_2 \varphi_l \rho}_{g(x,t)} \right) \frac{d\varphi_m}{dx}\, dx \\
\approx& -\chi_1 \frac{(\Delta x)^2}{4}\xi \left[\frac{d\varphi_m}{dx}\frac{d\varphi_l}{dx}\left(\frac{\partial c}{\partial x}(x_{j-1},t) + \frac{\partial c}{\partial x}(x_j,t) \right) \right. \\
& \left. + \frac{d\varphi_m}{dx}\left(\varphi_l(x_{j-1})\frac{\partial c^2}{\partial x^2}(x_{j-1},t) + \varphi_l(x_j)\frac{\partial^2 c}{\partial x^2}(x_j,t) \right) \right] \\
& + \frac{(\Delta x)^2}{4}\xi \frac{d\varphi_m}{dx}\left[g(x_{j-1},t)\varphi_l(x_{j-1}) + g(x_j,t)\varphi_l(x_j) \right],
\end{aligned}$$

where we have used Newton Côtes numerical integration. The element matrix now becomes

$$\begin{aligned}
S_p^{e_j} =& -\frac{\chi_1}{4}\xi \begin{pmatrix} \frac{\partial c}{\partial x}(x_{j-1},t) + \frac{\partial c}{\partial x}(x_j,t) & -\left(\frac{\partial c}{\partial x}(x_{j-1},t) + \frac{\partial c}{\partial x}(x_j,t)\right) \\ -\left(\frac{\partial c}{\partial x}(x_{j-1},t) + \frac{\partial c}{\partial x}(x_j,t)\right) & \frac{\partial c}{\partial x}(x_{j-1},t) + \frac{\partial c}{\partial x}(x_j,t) \end{pmatrix} \\
& + \frac{\chi_1}{4}\Delta x \xi \begin{pmatrix} \frac{\partial^2 c}{\partial x^2}(x_{j-1},t) & \frac{\partial^2 c}{\partial x^2}(x_j,t) \\ -\frac{\partial^2 c}{\partial x^2}(x_{j-1},t) & -\frac{\partial^2 c}{\partial x^2}(x_j,t) \end{pmatrix} \\
& + \frac{\Delta x}{4}\xi \begin{pmatrix} -g(x_{j-1},t) & -g(x_j,t) \\ g(x_{j-1},t) & g(x_j,t) \end{pmatrix}
\end{aligned} \tag{7.5.2}$$

As last we need to determine the extra term for the source vector.

$$\begin{aligned}
f_{p_m}^{e_j} =& \alpha_0 \frac{\Delta x}{2}\xi \int_{e_j} \rho(x,t)c(x,t)\frac{d\varphi_m}{dx}\, dx \\
\approx& \alpha_0 \frac{(\Delta x)^2}{4}\xi \frac{d\varphi_m}{dx}\left[\rho(x_{j-1},t)c(x_{j-1},t) + \rho(x_j,t)c(x_j,t) \right],
\end{aligned}$$

where we have used Newton côtes numerical integration. The element vector becomes

$$f_p^{e_j} = \alpha_0 \frac{\Delta x}{4}\xi \begin{pmatrix} -\left[\rho(x_{j-1},t)c(x_{j-1},t) + \rho(x_j,t)c(x_j,t)\right] \\ \rho(x_{j-1},t)c(x_{j-1},t) + \rho(x_j,t)c(x_j,t) \end{pmatrix}. \tag{7.5.3}$$

The mass matrix M_p, the stiffness matrix S_p and the source vector f_p are determined by (7.5.1)-(7.5.3). The matrices are tridiagonal matrices.
As last we need to know the value for ξ which is equal to the sign of the speed. Since the speed is given by $\chi_1 \frac{\partial c}{\partial x}$ we have $\xi = -1$.

With the obtained M_p, S_p, f_p and the matrices and vector from Chapter 6.2.3 the values for the capillary tip density can be determined when the equation is dominated by convergence.

Unfortunately, we did not yet obtain any results that showed the functionality of SUPG to our model.

Chapter 8

One dimensional discontinuous Galerkin method

Before we will apply the discontinuous Galerkin method [7] to our model as defined in Chapter 3, we first apply the method to the advection equation in order to practice the method.

For the discontinuous Galerkin method, we need to divide our domain into N elements. Each element is denoted as $e_j = [x_{j-1/2}, x_{j+1/2}]$ with $1 \leq j \leq N$ and element size Δ_j. The maximum element size is given by $\Delta x = \max_{1 \leq j \leq N} \Delta j$.

In order to derive the weak formulation we need to use test functions φ from the finite dimensional space

$$\Phi = \left\{ \varphi \in L^1(0,1) : \varphi|_{e_j} \in P^K(e_j),\ 1 \leq j \leq N \right\}, \tag{8.0.1}$$

where Φ is the space of all piecewise polynomials of degree (at most) K on element e_j.

As our basisfunctions we choose the Legendre polynomials since their L^2-orthogonality comes in a convenient manner for the treatment of our mass matrix. The nth Legendre polynomial is of order n. The first five Legendre polynomials are given in Table 8.0.1 and are also plotted in Figure 8.0.1.

$$\begin{aligned} P_0(r) &= 1 \\ P_1(r) &= r \\ P_2(r) &= \tfrac{1}{2}(3r^2 - 1) \\ P_3(r) &= \tfrac{1}{2}(5r^3 - 3r) \\ P_4(r) &= \tfrac{1}{8}(35r^4 - 30r^2 + 3) \end{aligned}$$

Table 8.0.1: *First five Legendre polynomials*

In order to use these Legendre polynomials, we redefine our weak formulation to a weak formulation on the scaled interval $[-1, 1]$ instead on our element interval $e_j = [x_{j-1/2}, x_{j+1/2}]$, this is often done by substituting $r = \frac{2(x-x_j)}{\Delta x}$.

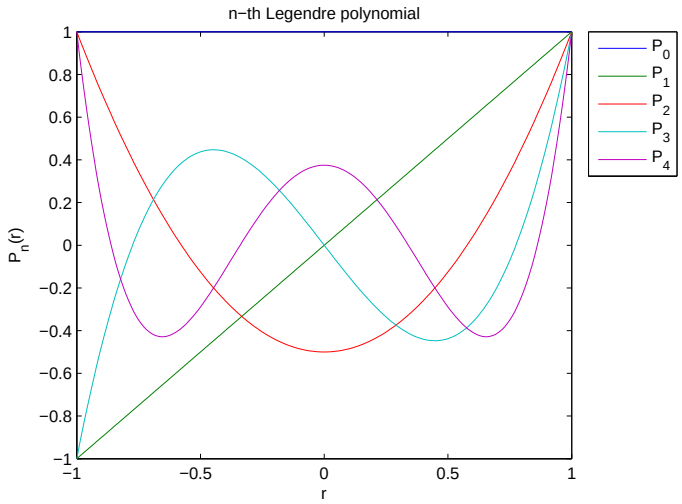

Figure 8.0.1: *The first five Legendre polynomials.*

With the discontinuous Galerkin method we get two (possibly) different solutions on the boundaries of all elements. One solution by the element left from the inter-element boundary and one solution by the element right from the inter-element boundary. Therefore we need to define a link between these two results. For the flux, we can use the central or the upwind flux.

8.1 Advection equation

We introduced the space of our test functions and the basisfunctions we use for each element e_j. Now we can approximate the solution to the advection equation. The advection equation is given by

$$\frac{\partial u}{\partial t} + \frac{\partial u}{\partial x} = 0, \ \forall x \in [0,1], \forall t \in [0,T], \tag{8.1.1}$$

$$u(x,0) = g(x), \ \forall x \in [0,1], \tag{8.1.2}$$

$$u(0,t) = u(1,t) = 0, \ \forall t \in [0,T], \tag{8.1.3}$$

with periodic boundary conditions.

The solution in element e_j is approximated by

$$u_h(x,t) = \sum_{l=0}^{K} u_j^l(t)\varphi_j^l(x), \tag{8.1.4}$$

where $\varphi^l(x) = P_l\left(\frac{2(x-x_j)}{\Delta x}\right)$ is the Legendre polynomial of lth order and $u_j^l(t)$ is the corresponding time-dependent coefficient.

8.1.1 Initial coefficients

First we need to determine the initial coefficients such that initial condition (8.1.2) applies. Therefore we multiply the initial condition by the test function $\varphi_j^m(x) \in \Phi$ and integrate it over the element e_j. By inserting (8.1.4), we obtain

$$\int_{e_j} u_h(x,0) P_m\left(\frac{2(x-x_j)}{\Delta x}\right)\, dx = \int_{e_j} \sum_{l=0}^{K} u_j^l(0) P_l\left(\frac{2(x-x_j)}{\Delta x}\right) P_m\left(\frac{2(x-x_j)}{\Delta x}\right)\, dx,$$
$$m \in \{0,\dots,K\},$$

where we subsitute $r = \frac{2(x-x_j)}{\Delta x}$ to obtain

$$\begin{aligned}\frac{\Delta x}{2}\int_{-1}^{1} u_h\left(\frac{\Delta x}{2}r + x_j, 0\right) P_m(r)\, dr &= \frac{\Delta x}{2}\sum_{l=0}^{K} u_j^l(0)\int_{-1}^{1} P_l(r)P_m(r)\, dr \\ &= \frac{\Delta x}{2}\frac{2}{2m+1}u_j^m(0),\ m \in \{0,\dots,K\}.\end{aligned}$$

Therefore the initial coefficients are given by

$$u_j^m(0) = \frac{2m+1}{2}\int_{-1}^{1} u_0\left(\frac{\Delta x}{2}r + x_j\right) P_m(r)\, dr,\ m \in \{0,\dots,K\}. \tag{8.1.5}$$

The initial coefficients given by (8.1.7) can be determined numerically using the Gauss-Legendre quadrature which read as

$$\int_{-1}^{1} f(x)\, dx \approx \sum_{i=1}^{p} w_i f(\hat{x}_i). \tag{8.1.6}$$

Here p denotes the number of points (and therefore also the number of weights) in which we need to evaluate the integrand. We choose to approximate the integral using six points. The points and the weights are listed in Table 8.1.1.

Points	Weights
± 0.23861918	0.46791393
± 0.66120939	0.36076157
± 0.93246951	0.17132449

Table 8.1.1: *Six points and their weights for the Gauss-Legendre quadrature*[1]

[1] `http://pathfinder.scar.utoronto.ca/~dyer/csca57/book_P/node44.html`

By substituting the points and their weights from Table 8.1.1 into Equation (8.1.5), we obtain

$$\begin{aligned} u_j^m(0) &= \frac{2m+1}{2} \int_{-1}^{1} u_0 \left(\frac{\Delta x}{2} r + x_j, 0 \right) P_m(r)\ dr \\ &\approx \frac{2m+1}{2} \sum_{i=1}^{6} u_0 \left(\frac{\Delta x}{2} r_i + x_j \right) P_m(r_i) w_i. \end{aligned} \tag{8.1.7}$$

8.1.2 Weak formulation

Once the initial coefficients are known, we determine the weak formulation for Equation (8.1.1). This is done by multiplying it by the testfunction $\varphi_j \in \Phi$ and integrating it over element e_j. We obtain

$$\int_{e_j} \frac{\partial u}{\partial t} \varphi_j + \frac{\partial u}{\partial x} \varphi_j\ dx = 0,$$

which becomes after partial integration

$$\int_{e_j} \frac{\partial u}{\partial t} \varphi_j - u \frac{d\varphi_j}{dx}\ dx + u\varphi_j|_{x_{j-1/2}}^{x_{j+1/2}} = 0.$$

Subsequently, we substitute Equation (8.1.4) into the above equation, and we set $\varphi_j = \varphi_j^m$ to obtain

$$\begin{aligned} \sum_{l=0}^{K} \frac{du_j^l}{dt} \underbrace{\int_{e_j} \varphi_j^l \varphi_j^m\ dx}_{M_{ml}} - \sum_{l=0}^{K} u_j^l \underbrace{\int_{e_j} \varphi_j^l \frac{d\varphi_j^m}{dx}\ dx}_{S_{ml}} \\ + u(x_{j+1/2}, t)\varphi_j^m(x_{j+1/2}) - u(x_{j-1/2}, t)\varphi_j^m(x_{j-1/2}) = 0. \end{aligned} \tag{8.1.8}$$

8.1.3 Mass matrix, element matrix and flux

Before we determine the mass matrix M_{ml}, the element matrix S_{ml} and the values on the boundaries we choose the number of Legendre polynomials we use. In this section we determine the matrices using two Legendre polynomials, so $K = 1$.

From the weak formulation (8.1.8), we know that the mass matrix M_{ml} equals

$$\begin{aligned} M_{ml} = \int_{e_j} \varphi_j^l(x) \varphi_j^m(x)\ dx &= \frac{\Delta x}{2} \int_{-1}^{1} P_l(r) P_m(r)\ dr \\ &= \frac{\Delta x}{2} \frac{2}{2m+1} \delta_{ml} \end{aligned}$$

where δ is the Kronecker delta. Hence

$$M = \Delta x \begin{pmatrix} 1 & 0 \\ 0 & \frac{1}{3} \end{pmatrix}, \tag{8.1.9}$$

The element matrix is given by

$$S_{ml} = \int_{e_j} \varphi_j^l(x) \frac{d\varphi_j^m}{dx}(x)\ dx = \int_{-1}^{1} P_l(r) \frac{dP_m}{dr}(r)\ dr.$$

Hence

$$S = \Delta x \begin{pmatrix} 0 & 0 \\ 2 & 0 \end{pmatrix}. \tag{8.1.10}$$

For the flux we use an upwind scheme and we insert Equation (8.1.4) into relation (8.1.8). Furthermore, we know that $\varphi_j^m(x_{j+1/2}) = P_m(1) = 1,\ \forall m$ and that $\varphi_j^m(x_{j-1/2}) = P_m(-1) = (-1)^m,\ m \in \{0, 1\}$. Therefore the boundary values are determined by

$$\begin{aligned} &u_h(x_{j+1/2}, t)\varphi_j^m(x_{j+1/2}) - u_h(x_{j-1/2}, t)\varphi_j^m(x_{j-1/2}) \\ &\qquad = \sum_{l=0}^{1} u_j^l(t)\varphi_j^l(x_{j+1/2}) - (-1)^m \sum_{l=0}^{1} u_{j-1}^l(t)\varphi_j^l(x_{j-1/2}),\ m \in \{0, 1\}. \end{aligned} \tag{8.1.11}$$

For the flux of the current cell and the flux of the previous cell we have two matrices, A and B, such that we have

$$A\mathbf{u}_j + B\mathbf{u}_{j-1},$$

with

$$A = \begin{pmatrix} 1 & 1 \\ 1 & 1 \end{pmatrix},\ B = -\begin{pmatrix} 1 & 1 \\ -1 & -1 \end{pmatrix} = \begin{pmatrix} -1 & -1 \\ 1 & 1 \end{pmatrix},\ \text{and } \mathbf{u}_\mathrm{j} = \begin{pmatrix} u_j^0 \\ u_j^1 \end{pmatrix}. \tag{8.1.12}$$

With equations (8.1.9), (8.1.10) and (8.1.12) we rewrite the weak formulation (8.1.8) into the follwing equation

$$M\frac{d\mathbf{u}_j}{dt} - S\mathbf{u}_j + A\mathbf{u}_j + B\mathbf{u}_{j-1} = 0,$$

which becomes using the Forward Euler time integration

$$M\mathbf{u}_j^{k+1} = (M + \Delta tS - \Delta tA)\mathbf{u}_j^k - \Delta tB\mathbf{u}_{j-1}^k, \tag{8.1.13}$$

where k denotes the time index at time t^k.

In order to determine the coefficients for the first element, e_1, we created a ghost cell on the left which is an exact copy of the most right element, element e_N. This can be done since we have periodic boundary conditions.

8.1.4 Results

We have the following exact solution to the inital boundary value problem defined in Equation (8.1.1)-(8.1.3) with $g(x) = \sin(2\pi x)$:

$$u(x,t) = \sin(2\pi(x-t)). \tag{8.1.14}$$

For comparison the exact solution is also shown in the figures where we show our approximations using the discontiuous Galerkin method. This is done by determining the exact solution for 10001 points with $\Delta x = 0.0001$ between the points.

In Figures 8.1.1 and 8.1.2 we respectively show the approximation using five and ten elements.

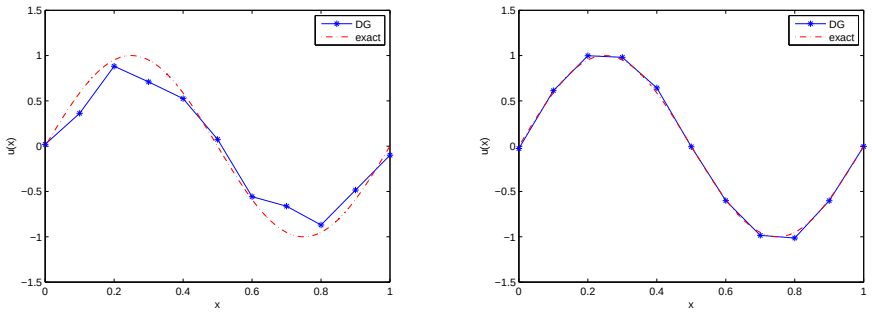

(a) Two Legendre polynomials (b) Three Legendre polynomials

Figure 8.1.1: *Results (two points per element) for the advection equation after* $t = 2$ *with five elements* ($\Delta x = 0.2$) *and* $\Delta t = 0.001$.

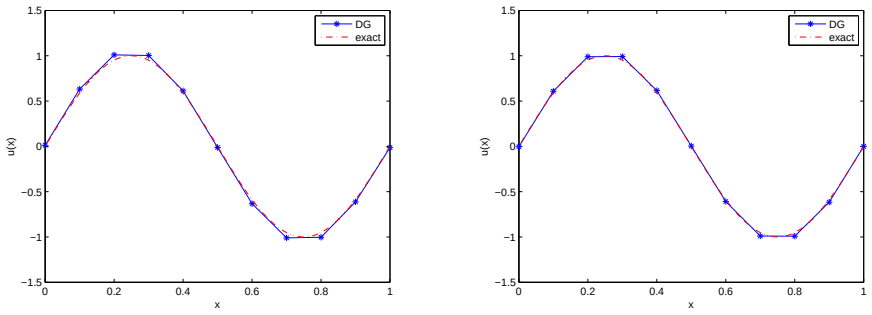

(a) Two Legendre polynomials (b) Three Legendre polynomials

Figure 8.1.2: *Results (one point per element) for the advection equation after* $t = 2$ *with ten elements* ($\Delta x = 0.1$) *and* $\Delta t = 0.001$.

Concentrating on Figure 8.1.1 it is clear that if we use three Legendre polynomials instead of two, the approximation gets more accurate. This can be explained since the third Legendre polynomial, the polynomial of order 2, is the first polynomial that is curved. So the third polynomial gives a significant contribution to the approximation of the curved exact solution given in Equation (8.1.14).

If we consider more elements, with smaller size, the exact solution will more and more look like a straight line on each element. Therefore, if we have a small enough elementsize, it is sufficient to just use two Legendre polynomials to get a good approximation. Figure 8.1.2 demonstrates this convergence since the solutions using two and three Legendre polynomials are very muck alike.

We also consider the approximation for a discontinuous initial condition. So we have our initial boundary value problem defined in (8.1.1)-(8.1.3) with

$$g(x) = \begin{cases} 5 & x \leq 0.5, \\ 0 & \text{elsewhere.} \end{cases} \tag{8.1.15}$$

The exact solution is given by

$$u(x,t) = 5H\left((0.5+t) - x\right). \tag{8.1.16}$$

In Figure 8.1.3 the approximations are shown for different choices of number of elements and the time step Δt. For these approximations we have always used only one Legendre polynomial, so we have basisfunctions of order zero. In Figure 8.1.3(a) we see that the solution with one Legendre polynomial is a good approximation to our exact solution. Here we have used a time step that is equal to the size of our elements. This means that the new solution of a cell e_j is exactly the old solution of the neighbouring cell e_{j-1}.

In Figure 8.1.3(b) we use a time step that is smaller than the size of our elements such that it satisfies the CFL condition. This means that after one time step, only a part of the solution of element e_{j-1} is shifted into element e_j. Therefore the new solution of element e_j will be a weighted average of the old solution of e_{j-1} and e_j. This also happens at the location of the discontinuity. Hence with $\Delta t < \Delta x$ numerical diffusion will occur.

The last situation is that the time step is larger than the size of our elements. In our case, where we have our speed equal to one, this means that the CFL condition is not satisfied. After one time step, the solution of element e_{j-1} is then multiple shifted to element e_j and wiggles will occur. This is shown in Figure 8.1.3(c).

We can also approximate the solution with higher order Legendre polynomials. This is done in Figure 8.1.4. Using a higher order approximation, in order to get stability, $\Delta t/\Delta x$ should be smaller than a certain value that depends on the order of the approximation and the order of the time integration method that is used. We used the Euler forwards time integration method (order one) and Legendre polynomials of order four. This means that $\Delta t/\Delta x$ should be smaller than zero, hence the approximation will never be stable.

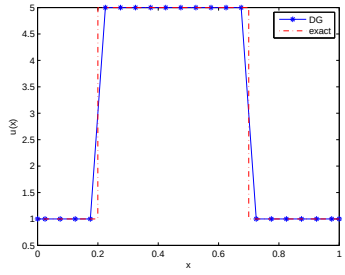

(a) With $\Delta x = 0.1$, $\Delta t = 0.1$ after $t = 0.25$

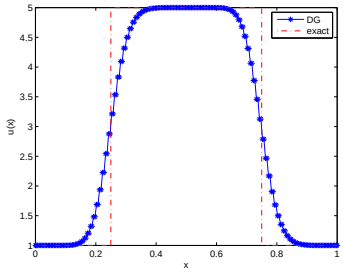

(b) With $\Delta x = 0.01$, $\Delta t = 0.001$ after $t = 0.25$

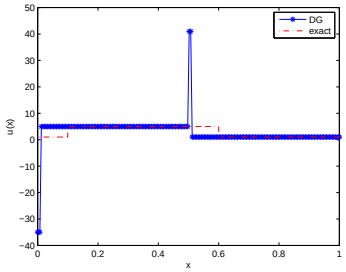

(c) With $\Delta x = 0.01$, $\Delta t = 0.1$ after $t = 0.1$

Figure 8.1.3: *Results (two points per element) using one Legendre polynomial for the advection equation with discontinuous initial condition.*

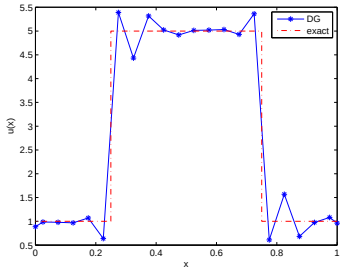

(a) With $\Delta x = 0.1$, $\Delta t = 0.001$ after $t = 0.25$

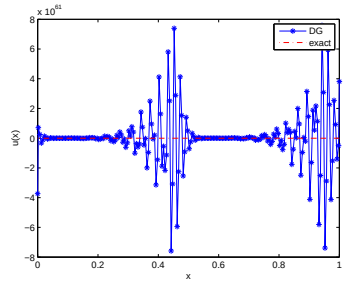

(b) With $\Delta x = 0.01$, $\Delta t = 0.001$ after $t = 0.25$

Figure 8.1.4: *Results (two points per element) using five Legendre polynomials for the advection equation with discontinuous initial condition.*

In Figure 8.1.4(a) we have $\Delta t/\Delta x = 0.01$ and some wiggles occur in the approximation. We can use a limiter to improve the approximation. In Figure 8.1.4(b) we have $\Delta t/\Delta x = 0.1$ which gives larger wiggles such that the approximation is clearly unstable. So we

should choose the Δx and Δt carefully.

8.1.5 Limiting

When using Legendre polynomials of higher order, limiting can be needed. In this chapter we apply limiting to the advection equation with discontinuous initial condition.

Minmod limiter

The minmod limiter is a limiter that is applied to the whole domain and it can be used for a polynomial basis P_0 or $P_0,\ P_1$, a basis of order 0 or 1. When we use a polynomial basis of a higher order we can still use the minmod limiter, but only where limiting is needed. In those elements the approximation will be reduced to order 1, while in the other elements the approximation is still of the higher order. To determine in which elements limiting is needed we should use some kind of detection. For now, we focus on a polynomial basis of order 1 so we can use the minmod limiter on the whole domain.

For the minmod limiter we need the minmod function which is given by

$$m(a,b,c) = \begin{cases} \text{sgn}(a)\cdot\min\{|a|,|b|,|c|\} & \text{if } \text{sgn}(a)=\text{sgn}(b)=\text{sgn}(c), \\ 0 & \text{elsewhere.} \end{cases} \tag{8.1.17}$$

For example, the minmod function is used in the monotonized central-difference limiter (van Leer [9]). We will use this limiter to improve the approximation to the advection equation. With this limiter the approximation $u_h(x,t^k)$ of the solution to element e_j, $j = 1 \dots N$, at t^k is given by

$$u_h(x,t^k) = \bar{u}_j^k + \sigma_j^k(x - x_j), \tag{8.1.18}$$

where $\bar{u}_j^k$ denotes the averaged approximation over element e_j. For $\bar{u}_j^k$ we obtain

$$\begin{aligned} \bar{u}_j^k =& \frac{1}{\Delta x}\int_{x_{j-\frac{1}{2}}}^{x_{j+\frac{1}{2}}} u_h(x,t^k)\ dx, \\ =& \frac{1}{\Delta x}\int_{x_{j-\frac{1}{2}}}^{x_{j+\frac{1}{2}}} \sum_{l=0}^{K} u_j^{(l)}(t^n) P_l \frac{2}{\Delta x}(x - x_j)\ dx \\ =& \frac{1}{\Delta x}\sum_{l=0}^{K} u_j^{(l)}(t^k)\cdot\frac{\Delta x}{2}\int_{-1}^{1} P_l(\xi)\ d\xi \\ =& u_j^{(0)}(t^k), \end{aligned} \tag{8.1.19}$$

since

$$\int_{-1}^{1} P_l(\xi)\ d\xi = \int_{-1}^{1} P_l(\xi)P_0(\xi)\ d\xi = \begin{cases} 2 & l = 0, \\ 0 & l \neq 0. \end{cases}$$

The slope σ_j^k for the Van Leer limiter is determined by

$$\sigma_j^k = m\left(\frac{\bar{u}_{j+1}^k - \bar{u}_{j-1}^k}{2\Delta x}, 2\frac{\bar{u}_j^k - \bar{u}_{j-1}^k}{\Delta x}, 2\frac{\bar{u}_{j+1}^k - \bar{u}_j^k}{\Delta x}\right). \tag{8.1.20}$$

For the advection equation (8.1.1) with discontinuous initial condition (8.1.2) defined in (8.1.15) we use a polynomial basis of order 1. Hence our solution after limiting is given by

$$\begin{aligned} u_h(x,t^k) =& \sum_{l=0}^{1} u_j^{(l)}(t^k) P_l(\xi) \\ =& u_j^{(0)} + u_j^{(1)} \frac{2}{\Delta x}(x - x_j) \\ =& u_j^{(0)} + \sigma_j^k (x - x_j). \end{aligned}$$

Therefore, when we use limiting, the renewed value equals

$$u_j^{(1)}(t^k) = \sigma_j^k \frac{\Delta x}{2}.$$

The algorithm that we applied for limiting the advection equation is as following:

Algorithm 1 Determine limited u^{k+1} with u^k

u^0 initial coefficients
$\bar{u}_{-1}^{(l)}(t^0) = \bar{u}_N^{(l)}(t^0)$;
$\bar{u}_{N+1}^{(l)}(t^0) = \bar{u}_0^{(l)}(t^0)$;
for $k = 1..Nt-1$ **do**
  for $j = 1..N$ **do**
    $in1 = (\bar{u}_{j+1}^{(l)}(t^k) - \bar{u}_{j-1}^{(l)}(t^k))/(2\Delta x)$;
    $in2 = 2 * (\bar{u}_j^{(l)}(t^k) - \bar{u}_{j-1}^{(l)}(t^k))/\Delta x$;
    $in3 = 2 * (\bar{u}_{j+1}^{(l)}(t^k) - \bar{u}_j^{(l)}(t^k))/\Delta x$;
    $\sigma = minmod(|in1|, |in2|, |in3|)$;
    $\bar{u}_j^{(1)}(t^k) = \sigma * \Delta x/2$; %Limited coefficient
  end for
  $\bar{u}_{-1}^{(l)}(t^k) = \bar{u}_N^{(l)}(t^k)$;
  $\bar{u}_{N+1}^{(l)}(t^k) = \bar{u}_0^{(l)}(t^k)$;
  Determine $\bar{u}^{(l)}(t^{k+1})$ with Euler Forward
  $\bar{u}_{-1}^{(l)}(t^{k+1}) = \bar{u}_N^{(l)}(t^{k+1})$;
  $\bar{u}_{N+1}^{(l)}(t^{k+1}) = \bar{u}_0^{(l)}(t^{k+1})$;
  Determine solution $u_h(x,t^k)$ with limited coefficients
end for

Results

In Figure 8.1.5 the results are shown for the advection equation with discontinuous initial condition using only ten elements and a polynomial basis of order 1. The same is shown in Figure 8.1.6 with 100 elements. Both with an other time step in order to satisfy the CFL condition. In both figures the results without limiting are bad. Wiggles start to occur, especially when we have 100 elements. When using the limiter described before, the wiggles seem to be gone and the approximations are more accurate. Especially when we use 100 elements.

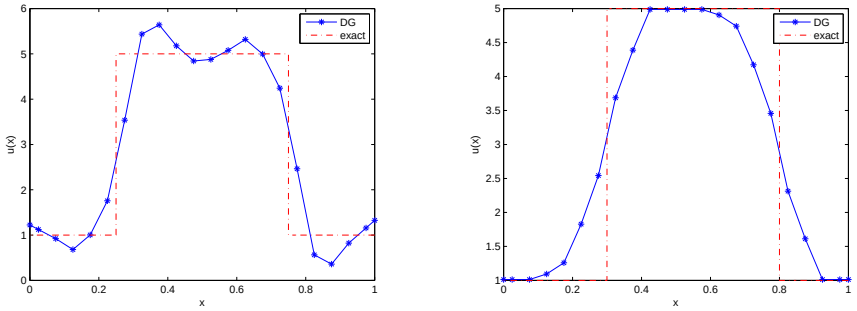

(a) Without limiting (b) With limiting

Figure 8.1.5: *Results (two points per element) using two Legendre polynomials (up to order $K = 1$) for the advection equation with discontinuous initial condition, using $\Delta x = 0.1$, $\Delta t = 0.01$ and $t = 0.25$.*

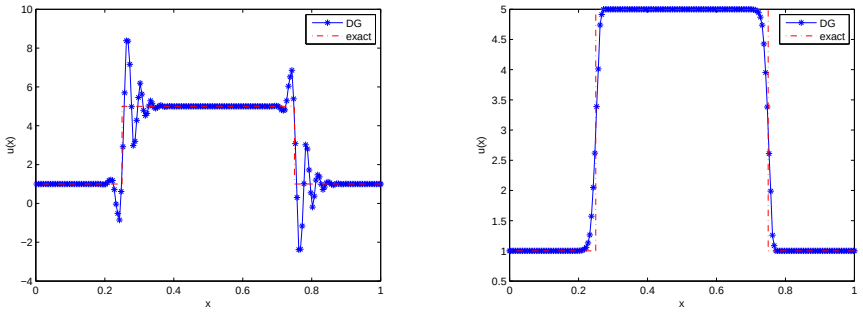

(a) Without limiting (b) With limiting

Figure 8.1.6: *Results (two points per element) using two Legendre polynomials (up to order $K = 1$) for the advection equation with discontinuous initial condition, using $\Delta x = 0.01$, $\Delta t = 0.001$ and $t = 0.25$.*

Chapter 9

Discussion and further research

In the previous chapters we have shown results for the angiogenesis model using different numerical methods. In order to obtain the results we used the parameter values that were also used in [2]. The parameter values we needed for the stem cell density have been chosen based on educational guesses. The question is whether or not these parameter values are realistic. Therefore, the choice of the values needs some discussion in the upcoming research.

During the literature study, our model was only one dimensional. In our further research we will extend the model into two dimensions.

The following research questions and goals, are the topics that will be treated during the rest of my research:

For the model:

- Expand the model to two dimensions.
- Apply the finite element method to our 2D model.
  To learn how angiogenesis works in two dimensions.
- Are the values of the parameters realistic?
- Are the initial conditions of the several densities realistic?

Involving DG:

- How can we limit the approximation using higher order basic functions?
  How can we detect wiggles and smearing such that we know where to apply the minmod limiter when we apply discontinuous Galerkin?
- Apply discontinuous Galerkin to our 1D model.
  Limit if necessary.
- Apply discontinuous Galerkin to the 2D advection equation.
  In order to get familiar with DG for a two dimensional problem.

- Apply discontinuous Galerkin to our 2D model.
  Limit if nexessary.

Research question:

- How many stem cells should be injected when aiming at avoiding the formation of scar tissue?
  Is the amount of stem cells compensating for the loss term?

Appendix A

Calculations with the hyperbolic sine and cosine

A.1 Integral of the hyperbolic sine

Integral 1

$$\begin{aligned}\int \frac{1}{\sinh(x)}dx =& 2\int \frac{1}{e^x - e^{-x}}dx \\ =& 2\int \frac{e^x}{e^{2x}-1}dx \\ \overset{u=e^x}{=}& 2\int \frac{1}{u^2-1}du \\ =& 2\int \frac{A}{u+1} + \frac{B}{u-1}du. \end{aligned} \tag{A.1.1}$$

To determine A and B we get

$$\begin{aligned} &A(u-1) + B(u+1) = 1, \\ &(A+B)u + B - A = 1, \\ &\Rightarrow\ A + B = 0\ \Rightarrow\ A = -B, \\ &\Rightarrow\ B + B = 1\ \Rightarrow\ B = 1/2\ \Rightarrow\ A = -1/2. \end{aligned} \tag{A.1.2}$$

With A and B from (A.1.2), Equation (A.1.1) becomes

$$\begin{aligned}\int \frac{1}{\sinh(x)}dx =& 2\int \frac{1/2}{u-1} - \frac{1/2}{u+1}du = \int \frac{1}{u-1} - \frac{1}{u+1}du \\ =& \ln(u-1) - \ln(u+1) = \ln\left(\frac{u-1}{u+1}\right) = \ln\left(\frac{e^x-1}{e^x+1}\right) \\ =& \ln\left(\tanh\left(\frac{x}{2}\right)\right). \end{aligned} \tag{A.1.3}$$

Analogously, the solution for

$$\int \frac{1}{\sinh(\gamma x)} dx,$$

is given by

$$\begin{aligned}\int \frac{1}{\sinh(\gamma x)} dx =& \frac{1}{\gamma} \int \frac{1}{\sinh(y)} dy = \frac{1}{\gamma} \ln\left(\tanh\left(\frac{y}{2}\right)\right) \\ =& \frac{1}{\gamma} \ln\left(\tanh\left(\frac{\gamma x}{2}\right)\right). \end{aligned} \tag{A.1.4}$$

Integral 2
A little more difficult is the following integral:

$$\begin{aligned}\int \frac{1}{A\sinh(y) - B\cosh(y)} dy =& 2\int \frac{1}{A(e^y - e^{-y}) - B(e^y + e^{-y})} dy \\ =& 2\int \frac{1}{(A-B)e^y - (A+B)e^{-y}} dy \\ =& 2\int \frac{e^y}{(A-B)e^{2y} - (A+B)} dy \\ =& \frac{2}{A-B}\int \frac{e^y}{e^{2y} - \frac{A+B}{A-B}} dy \overset{u=e^y}{=} \frac{2}{A-B}\int \frac{1}{u^2 - \frac{A+B}{A-B}} du. \\ \overset{z=\frac{A+B}{A-B}}{=}& \frac{2}{A-B}\int \frac{\alpha}{u+\sqrt{z}} + \frac{\beta}{u-\sqrt{z}} du \end{aligned}$$

To determine α and β we get

$$\begin{aligned}&\alpha(u-1) + \beta(u+1) = 1, \\ &(\alpha+\beta)\beta - \alpha = 1, \\ &\Rightarrow\ \alpha + \beta = 0\ \Rightarrow\ \alpha = -\beta, \\ &\Rightarrow\ \beta + \beta = 1\ \Rightarrow\ \beta = \frac{1}{2\sqrt{z}}\ \Rightarrow\ \alpha = -\frac{1}{2\sqrt{z}}. \end{aligned} \tag{A.1.5}$$

Substituting this solution, we obtain

$$\begin{aligned}\frac{2}{A-B}\int \frac{\alpha}{u+\sqrt{z}} + \frac{\beta}{u-\sqrt{z}} du =& \frac{2}{A-B}\int \frac{\frac{1}{2\sqrt{z}}}{u-\sqrt{z}} - \frac{\frac{1}{2\sqrt{z}}}{u+\sqrt{z}} du \\ =& \frac{1}{\sqrt{A^2-B^2}}\left[\ln\left(u-\sqrt{z}\right) - \ln\left(u+\sqrt{z}\right)\right]. \end{aligned}$$

Redo the substitutions that were made, we obtain

$$\int \frac{1}{A\sinh(y) - B\cosh(y)} dy = \frac{1}{\sqrt{A^2-B^2}} \ln\left(\frac{e^y - \sqrt{\frac{A+B}{A-B}}}{e^y + \sqrt{\frac{A+B}{A-B}}}\right).$$

Integral 3
More difficult is the next integral

$$\int \frac{dv}{\gamma \sinh(v) + \sinh(v-w)} = \frac{1}{\gamma}\int \frac{dv}{\sinh(v) + \frac{1}{\gamma}\sinh(v-w)},$$

where we gonna substitute $A = \frac{1}{\gamma}e^{-w}$ and $B = \frac{1}{\gamma}e^{w}$ to obtain

$$\begin{aligned}
\frac{1}{\gamma}\int \frac{dv}{\sinh(v) + \frac{1}{\gamma}\sinh(v-w)} &= \frac{2}{\gamma}\int \frac{dv}{(e^v - e^{-v}) + \frac{1}{\gamma}(e^{v-w} - e^{-(v-w)})} \\
&= \frac{2}{\gamma}\int \frac{1}{(e^v - e^{-v}) + Ae^v - Be^{-v}}dv \\
&= \frac{2}{\gamma}\int \frac{1}{e^v(A+1) - e^{-v}(B+1)}dv \\
&= \frac{2}{\gamma}\int \frac{e^v}{e^{2v}(A+1) - (B+1)}dv \\
&\overset{u=e^v}{=} \frac{2}{\gamma}\int \frac{1}{u^2(A+1) - (B+1)}du \\
&= \frac{2}{\gamma}\frac{1}{A+1}\int \frac{1}{u^2 - \frac{B+1}{A+1}}du,
\end{aligned}$$

which equals, using (A.1.5),

$$\begin{aligned}
\frac{1}{\gamma}\int \frac{dv}{\sinh(v) + \frac{1}{\gamma}\sinh(v-w)} &= \frac{2}{\gamma}\frac{1}{A+1}\int \frac{-\frac{1}{2}\sqrt{\frac{A+1}{B+1}}}{u + \sqrt{\frac{B+1}{A+1}}} + \frac{\frac{1}{2}\sqrt{\frac{A+1}{B+1}}}{u - \sqrt{\frac{B+1}{A+1}}}du \\
&= \frac{1}{\gamma}\frac{1}{A+1}\int \frac{-\sqrt{\frac{A+1}{B+1}}}{u + \sqrt{\frac{B+1}{A+1}}} + \frac{\sqrt{\frac{A+1}{B+1}}}{u - \sqrt{\frac{B+1}{A+1}}}du \\
&= \frac{1}{\gamma}\frac{1}{\sqrt{(A+1)(B+1)}}\int \frac{1}{u - \frac{B+1}{A+1}} - \frac{1}{u + \sqrt{\frac{B+1}{A+1}}}du \\
&= \frac{1}{\gamma}\frac{1}{\sqrt{AB+A+B+1}}\ln\left(\frac{u - \sqrt{\frac{B+1}{A+1}}}{u + \sqrt{\frac{B+1}{A+1}}}\right) \\
&= \frac{1}{\gamma}\frac{1}{\sqrt{AB+A+B+1}}\ln\left(\frac{e^v - \sqrt{\frac{B+1}{A+1}}}{e^v + \sqrt{\frac{B+1}{A+1}}}\right). \qquad \text{(A.1.6)}
\end{aligned}$$

A.2 Rewriting some terms

We know that

$$\sinh\left(\sqrt{\tilde{\lambda}}(1-\delta)\right) = \sinh\left(\sqrt{\tilde{\lambda}}x\right)\cosh\left(\sqrt{\tilde{\lambda}}\delta\right) - \cosh\left(\sqrt{\tilde{\lambda}}x\right)\sinh\left(\sqrt{\tilde{\lambda}}\delta\right),$$

such that

$$
\begin{aligned}
&- \frac{\sinh\left(\sqrt{\tilde{\lambda}}(1-\delta)\right)}{\sinh\left(\sqrt{\tilde{\lambda}}\right)} + \cosh\left(\sqrt{\tilde{\lambda}}\delta\right) \\
&= \frac{-\sinh\left(\sqrt{\tilde{\lambda}}\right)\cosh\left(\sqrt{\tilde{\lambda}}\delta\right) + \cosh\left(\sqrt{\tilde{\lambda}}\right)\sinh\left(\sqrt{\tilde{\lambda}}\delta\right)}{\sinh\left(\sqrt{\tilde{\lambda}}\right)} + \cosh\left(\sqrt{\tilde{\lambda}}\delta\right) \\
&= \frac{\cosh\left(\sqrt{\tilde{\lambda}}\right)\sinh\left(\sqrt{\tilde{\lambda}}\delta\right)}{\sinh\left(\sqrt{\tilde{\lambda}}\right)} = \frac{\sinh\left(\sqrt{\tilde{\lambda}}\delta\right)}{\tanh\left(\sqrt{\tilde{\lambda}}\right)}.
\end{aligned}
$$

Bibliography

[1] *www.hartaanval.nl*

[2] H. M. Byrne and M. A. J. Chaplain, *Explicit Solutions of a Simplified Model of Capillary Sprout Growth During Tumor Angiogenesis* School of Mathematical Sciences, University of Bath. Claverton Down, Bath BA2 7AY, U.K. 1995

[3] L.Y.D. Crapts, *A mathematical model for angiogenesis around a tumour* Bachelor of Science thesis, Delft Technical University, June 2010.

[4] J. van Kan, A. Segal, and F. Vermolen, *Numerical Methods in Scientific Computation* VSSD, 2008.

[5] Sophia A. Maggelakis, *A mathematical model of tissue replacement during epidermal wound healing* Applied Mathematical Modelling 27 (2003) 189196

[6] Sophia A. Maggelakis, *Modeling the role of angiogenesis in epidermal wound healing* Discrete and continuous dynamical systems-series B, Volume 4, Number 1, February 2004

[7] Jan S. Hesthaven, *Nodal Discontinuous Galerkin Methods* Springer 2008.

[8] Henri Paillere, *Multidimensional upwind residual distribution schemes for the euler and navier-stokes equations on unstructured meshes*

[9] Randall J. Leveque, *Finite Volume Methods for Hyperbolic Problems* Cambridge Texts in Applied Mathematics. Cambridge University Press, New York, sixth edition, 2002.